

ED NO. 20216
ASTIA FILE COPY

**ULTRASONIC AND ELECTROCHEMISTRY
RESEARCH LABORATORY**

Department of Chemistry
WESTERN RESERVE UNIVERSITY
Cleveland, Ohio

ULTRASONICS AND ELECTROCHEMISTRY

REPRODUCED

FROM

**LOW CONTRAST COPY.
ORIGINAL DOCUMENTS
MAY BE OBTAINED ON
LOAN**

FROM

**ARMED SERVICES TECHNICAL INFORMATION AGENCY
DOCUMENT SERVICE CENTER
KNOTT BUILDING, DAYTON 2, OHIO**

**Parts of this document
are not reproducible**

THE FREQUENCY CHARACTERISTICS OF ACOUSTO-
ELECTROCHEMICAL EFFECTS: THE ELECTROKINETIC
AND POLARIZED GAS ELECTRODE EFFECTS

Technical Report No. 13

by

Frank Saunders, Ernest Yeager, and Frank Hovorka

ULTRASONIC RESEARCH LABORATORY

Department of Chemistry

WESTERN RESERVE UNIVERSITY

Cleveland 6, Ohio

1 September 1953

Office of Naval Research
Contract No. N7 onr 47002
Project No. 384 305

TABLE OF CONTENTS

TABLE OF CONTENTS

	Page
Abstract	11
A. Introduction	1
B. Previous Work on the Electrokinetic Effect at 200 kc./sec.	2
C. Previous Work on the A.C. Polarized Gas Electrode Effect at 200 kc./sec	4
D. The Frequency Characteristics of the Acousto- Electrokinetic Effect	5
1. Method of Measurement	5
2. Experimental Results	8
3. Interpretation and Conclusions	21
E. The Frequency Dependence and Related Characteristics of the A.C. Polarized Gas Electrode Effect	25
1. Experimental Techniques	25
2. Experimental Results	28
3. Interpretation and Conclusions	39
APPENDIX: Instrumentation for the Determination of the Frequency Dependence of the Acousto-Electrochemical Effects	42
Distribution List	62

THE FREQUENCY CHARACTERISTICS OF ACOUSTO-
ELECTROCHEMICAL EFFECTS: THE ELECTROKINETIC
AND POLARIZED GAS ELECTRODE EFFECTS

Technical Report No. 13

by

Frank Saunders, Ernest Yeager, and Frank Hovorka

- ABSTRACT -

The frequency characteristics of the acousto-electrokinetic effect (Technical Report No. 5) and the a.c. polarized gas electrode effect (Technical Report No. 8) have been determined relative to solution and electrode parameters. Measurements with pulse-modulated ultrasonic waves in the range 200 to 1000 kc./sec. indicate that in the case of the electrokinetic effect the response in terms of pressure amplitude is inversely proportional to the frequency in very dilute solutions. This frequency dependence becomes less marked with increasing conductance of the solutions. The polarized gas electrode effect has been studied with hydrogen gas in the same frequency range. The response also decreases with increasing frequency although the extent of the decrease is a function of the current density and specific conductance. Both the response and stability of the polarized gas electrode effect have been greatly improved by the use of a directed flow solution

past the electrode to remove the cloud of gas bubbles in the bulk of the solution surrounding the electrode. Current interruptor techniques have also been applied to the study of the a.c. response of the hydrogen electrode. Audio modulated polarizing currents have been examined as a means for eliminating electro-magnetic coupling problems.

The mechanisms proposed for the electrokinetic effect and the polarized gas electrode effect in earlier reports have been further substantiated by the present work.

THE FREQUENCY CHARACTERISTICS OF ACOUSTO-
ELECTROCHEMICAL EFFECTS: THE ELECTROKINETIC
AND POLARIZED GAS ELECTRODE EFFECTS

Technical Report No. 13

1 September 1953

A. INTRODUCTION

Previous technical reports¹⁻⁴ and publications⁵⁻⁸ have described the characteristics of the electrokinetic effect^{2,7} and the a.c. polarized gas electrode effect^{1,3,8} at a frequency of 200 kc./sec. The present report is concerned with the frequency dependence of these

-
1. Technical Report No. 3, "The Effect of Acoustical Radiations on the Hydrogen Electrode (theory)", Ultrasonics Research Laboratory, Western Reserve University, 1950.
 2. Technical Report No. 5, "An Electrokinetic Probe for the Detection of Ultrasonic Waves", *ibid.*, 1951.
 3. Technical Report No. 8, "The Production of Alternating Components in the Potential of a Polarized Hydrogen Electrode", *ibid.*, 1952.
 4. Technical Report No. 11, "A Survey of the Electrochemical Applications of Ultrasonic Waves", *ibid.*, 1953.
 5. Yeager and Hovorka, *J. Electrochem. Soc.*, 98, 14 (1951).
 6. Yeager and Hovorka, *J. Acoust. Soc. Am.*, 25, 443 (1953).
 7. Dietrick, Yeager, Bugosh, and Hovorka, *ibid.*, 25, 461 (1953).
 8. Dietrick, Yeager, Bugosh, and Hovorka, *ibid.*, 25, 466 (1953).

effects. In the case of the polarized gas electrode effect, additional measurements involving directional flow of the electrolytic solution and the use of current interruption techniques have resulted in a more complete interpretation of the effect.

Before describing the new measurements, the previous work at 200 kc./sec. will be briefly reviewed.

B. PREVIOUS WORK ON THE ELECTROKINETIC EFFECT AT 200 KC./SEC.

If a wire with a porous or fibrous covering is placed in a dilute electrolytic solution and exposed to ultrasonic waves, an alternating potential of the same frequency is produced on the central conductor relative to the bulk of the surrounding solution. The effect was first noted⁹ at 200 kc./sec. with a cotton-covered copper wire probe; hence, it has been often referred to as the "cotton-covered copper wire" effect. The cotton covering, however, is by no means unique.

The investigation of the effect at 200 kc./sec. has involved the use of pulse-modulated ultrasonic waves and apparatus described elsewhere¹⁰. Pulse-techniques eliminate any possible difficulties associated with electromagnetically induced effects and at the same time are conducive to quantitative acoustical measurements in tanks of limited dimensions. The

9. Bugosh, Yeager, and Hovorka, Phys. Rev., 76, 1891 (1949).

10. Technical Report No. 2, "Apparatus for Acoustical Measurements with Pulse-Modulated Ultrasonic Waves", 1949.

following information has been obtained through these measurements:

1. The effect is dependent on the presence of a porous covering.
2. The effect is independent of the base metal.
3. The relative dependence of the effect on the type and the concentration of the electrolyte, the pH, and the type of porous covering is essentially the same as the dependence of d.c. streaming potentials on the same parameters.
4. The amplitude of the observed effect is a linear function of the pressure amplitude of the ultrasonic waves in a progressive field.
5. The frequency of the a.c. potentials is the same as that of the ultrasonic waves. The harmonic content is negligible.
6. The effect is very reproducible and has virtually no time dependence after the electrolyte has wet the fibers.
7. Under favorable conditions the effect may be as large as -145 db.re.: 1 volt per dyne/cm².

Theoretical considerations of the effect have been based on an electrokinetic mechanism, an assumption which is well supported by the experimental results. The effect depends on an a.c. displacement or distortion of the diffuse layer of ions surrounding each fiber. On the basis of this mechanism, the amplitude of the effect should be directly dependent on the zeta potential and the conductance of the solution in a manner similar to that for d.c. streaming potentials. This a.c. electrokinetic effect is analogous to the colloidal vibration potentials¹¹.

The experimental work at 200 kc./sec. also has indicated that this effect can be used to follow zeta-potential changes on fibers. Another application is the utilization of the electrokinetic effect in the form

11. Technical Report No. 7, "Colloidal Vibration Potentials", 1952.

of a high frequency acoustical probe of very small dimensions.

C. PREVIOUS WORK ON THE A.C. POLARIZED GAS ELECTRODE EFFECT

If acoustical waves are allowed to impinge upon an electrode at which gas is being liberated by electrolysis, an alternating component of the same frequency is developed on the wire relative to the bulk of the solution. The effect has been investigated at 200 kc./sec. with pulse-modulated ultrasonic waves in the case of the polarized hydrogen cathode. The experimental techniques are very similar to those used in the work on the electrokinetic effect.

The following are the results of the experimental work at 200 kc./sec.:

1. The effect is dependent on the formation of gas bubbles by electrolysis. The magnitude of the a.c. response is less by a factor of 10 to 100 for a polarized non-gaseous electrode under similar circumstances.
2. The effect is dependent on the polarizing current. A negligible effect has been found for the reversible hydrogen electrode at 200 kc./sec. in the absence of a polarizing current. The observed response is linearly dependent on the current density at low values of the latter. A complex dependence has been noted at higher current densities ($> 100 \text{ ma./cm}^2$.) with several plateaus evident.
3. At low current densities, the amplitude of the effect is approximately inversely proportional to the conductance of the solution.
4. The effect is essentially independent of pH and the type of electrolyte provided only hydrogen ions are discharged at the cathode and the conductance is held constant.
5. The effect is independent of the type of metal used as a cathode for practical purposes although the results are more reproducible with platinized-platinum cathodes.
6. Under favorable conditions the effect may be as large as -150 db. re.: 1 volt per dyne/cm^2 .

The effects of acoustical radiations on the reversible and polarized hydrogen electrodes have been considered theoretically in terms of a

thermodynamic treatment,¹² which is applicable only at very low frequencies, and a kinetic treatment⁵. The latter supports the conclusion that ultrasonically produced perturbations in the electrode reactions result in only a very minor contribution to the observed response at frequencies as high as 200 kc./sec. The prime mechanism for the effect is probably the modulation of the IR drop in the immediate vicinity of the electrode surface by periodically expanding and contracting gas bubbles. The experimental results at 200 kc./sec. support this conclusion.

The a.c. polarized gas electrode effect offers possibilities as a means for studying bubble formation at gas electrodes and can also be used for laboratory measurements of acoustical amplitude.

D. THE FREQUENCY CHARACTERISTICS OF THE ACOUSTO-ELECTROKINETIC EFFECT

1. Method of Measurement:

The frequency dependence of the acousto-electrokinetic effect has been determined in the frequency range from 200 kc./sec. to 1 mc./sec. The frequency dependence has been studied relative to variations in concentration of sodium chloride solutions, wire length, and coverings. The electronic and acoustical propagation apparatus employed for this work is described in the appendix of this report. The measurements have been made with a pulse-repetition frequency of 300 sec.⁻¹ at a pulse duration of 400 microseconds for the pulse modulation of the ultrasonic carrier. The pressure amplitude of the ultrasonic waves has been determined in the

12. Yeager and Hovorka, J. Chem. Phys., 17, 416(1949).

acoustical cell with a 1/8-in. barium titanate hydrophone. This hydrophone has been calibrated by comparison with a similar unit which in turn had been calibrated by the U.S. Navy Underwater Sound Reference Laboratory at Orlando. The probable error of the amplitude measurements is estimated to be ± 1 db. although the precision at a particular frequency is a fraction of this value.

The construction of the electrokinetic probe is shown in Figure 1. The acoustically sensitive element was mounted with deKhotinsky cement in the capillary tip drawn at the end of a glass tube. The exposed end of the wire was sealed with a small ball of the same cement to prevent direct contact with the solution. A brass probe housing served as shielding for the central conducting wire and electrical connection was made with a single microphone connector. The length of the wire exposed to the solution was either 1.5 cm. or 0.5 cm. The alternating components were measured on the central conducting wire relative to ground since the solution was essentially at a.c. ground because of the large capacity between the solution and ground.

The following procedure was used in the preparation of the electrokinetic probes for acoustical measurements. The probes were constructed as shown in Figure 1 using commercial copper wire with the prescribed coverings. Before any measurements were recorded on the various probes, the probes were allowed to stand in the solution for approximately one hour to ensure complete wetting of the fibrous covering. The values recorded in the following figures represent the mean values for several probes of the same construction. The deviation in response is approximately 1 db. from the mean for probes of the same type.

Sodium chloride solutions of various concentrations have been used

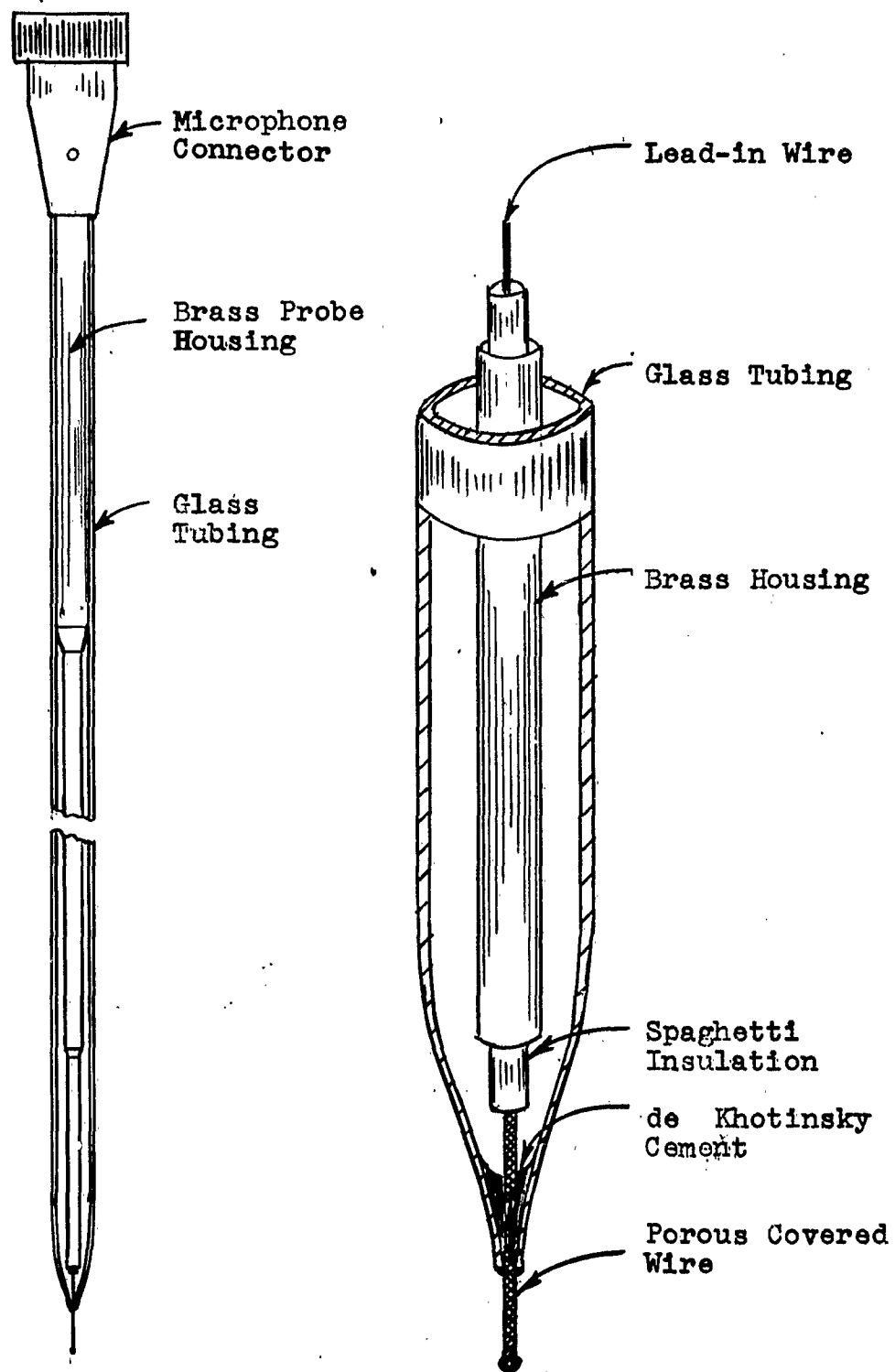


Figure 18

Electrokinetic Probe

in all cases and formulated directly in the acoustical cell by additions of reagent grade sodium chloride to distilled water in the cell. The solutions were made in order of increasing concentration with the concentration determined by conductance measurements after each run. In the case of the cotton coverings, previous work at 200 kc./sec. has indicated⁵ a negligible dependence on pH in the range 4 to 8; hence, it was not necessary to control this variable provided it was in this range.

2. Experimental Results:

In Figures 2-4 is represented graphically the frequency dependence of the electrokinetic effect for double cotton-covered copper wire (30 gage, B, and S.) in sodium chloride solutions of various concentrations. The solid lines in each graph indicate the terminated response in db. re.: 1 volt per dyne/cm². with the effect loaded by the impedance associated with the probe housing as well as the input impedance of the cathode-follower preamplifier. The dotted lines represent the open-circuit responses calculated from impedance measurements². The magnitude of the parallel resistive-capacitive components has been determined with a General Radio twin-T impedance bridge, Model 921A. The components of the load impedance have been measured between the central conductor of the probe and ground with the probe out of the solution. The difference between this impedance and the value with the probe submerged in the solution has been assumed to be associated with the effective internal impedance for the effect. The components of the load and internal impedance for the 0.5-cm. and 1.5-cm. probes in different concentrations of sodium chloride are given in Table 1 as a function of

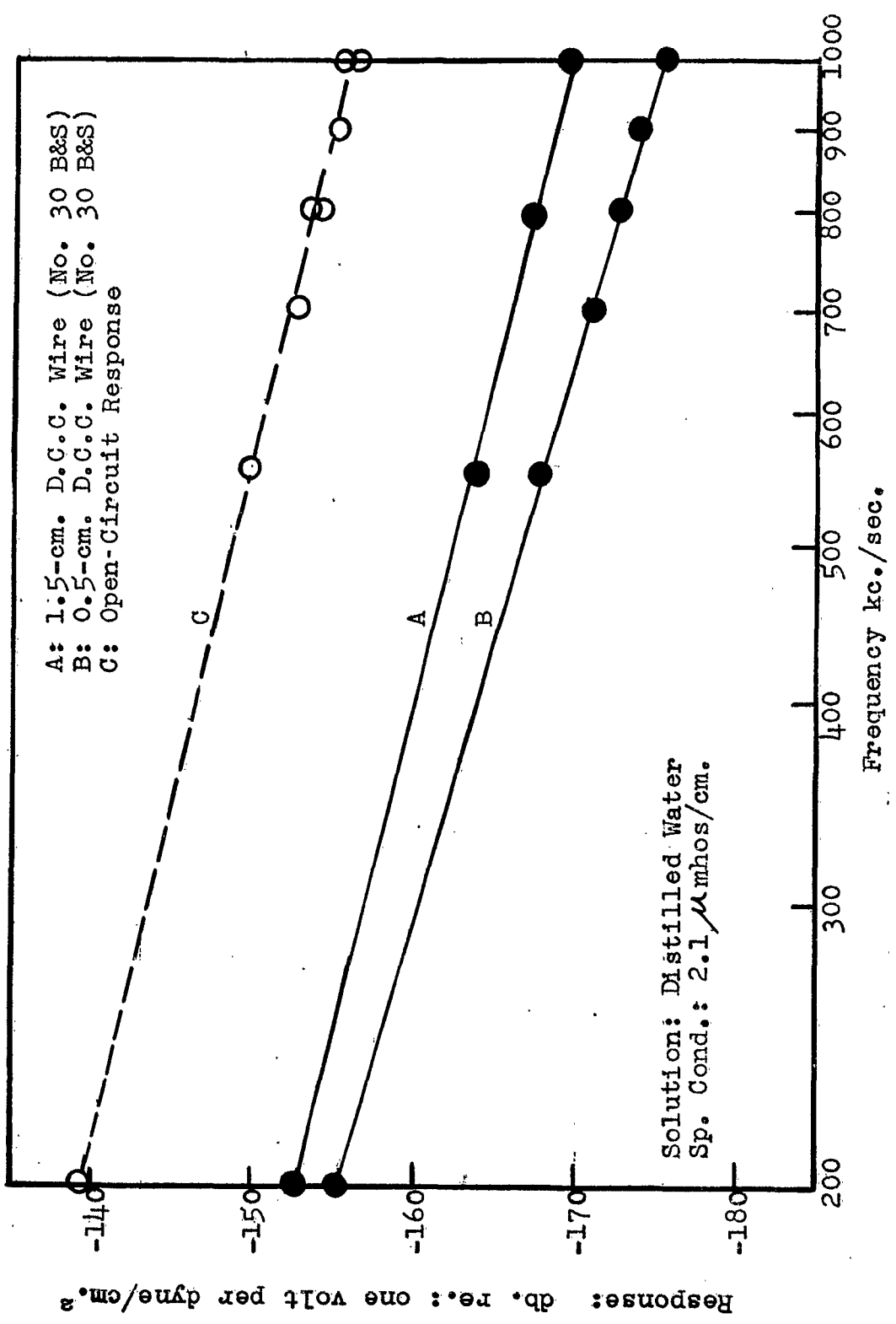


Figure 2: Dependence of Electrokinetic Effect on Frequency in Distilled Water.

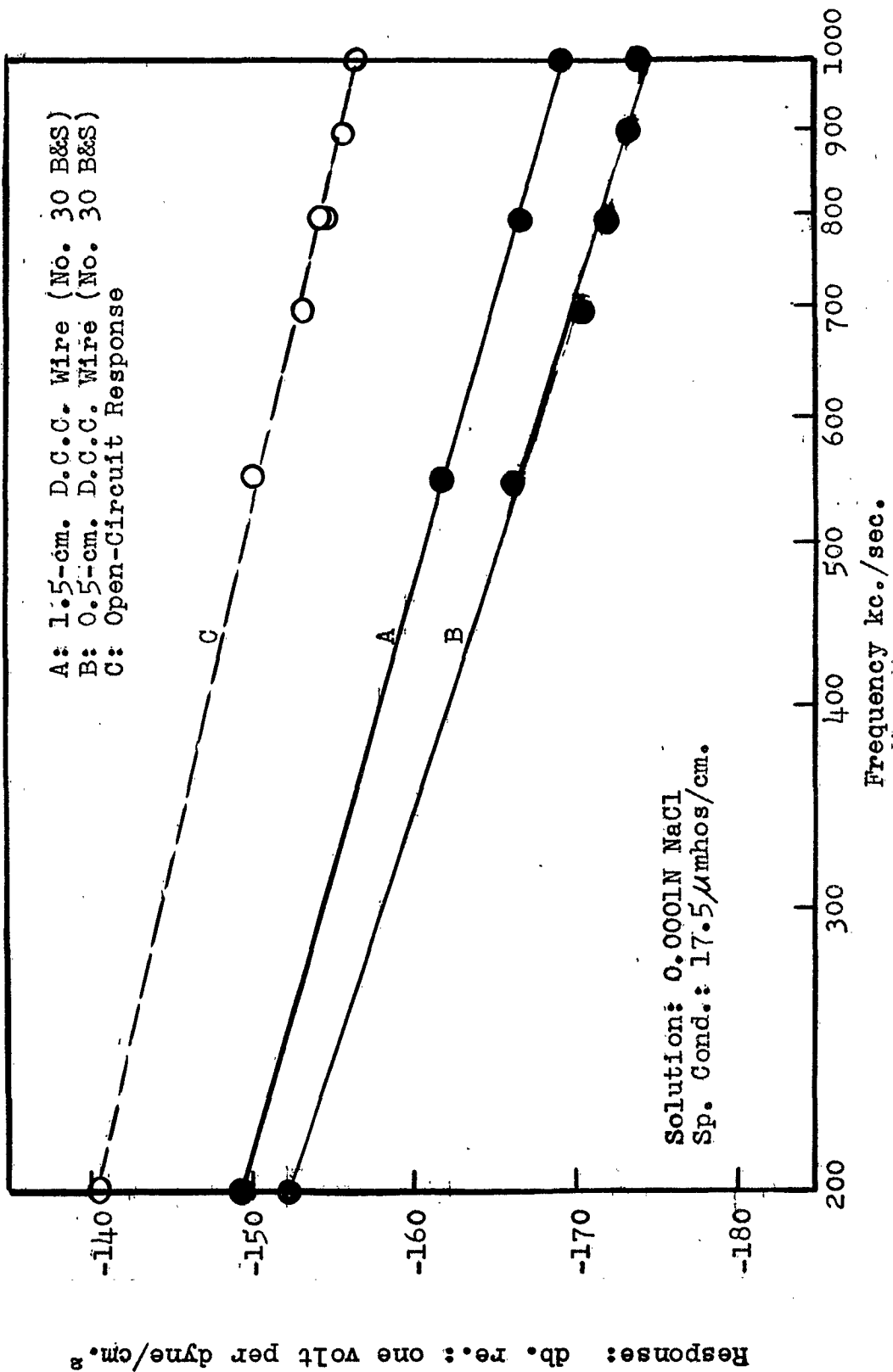
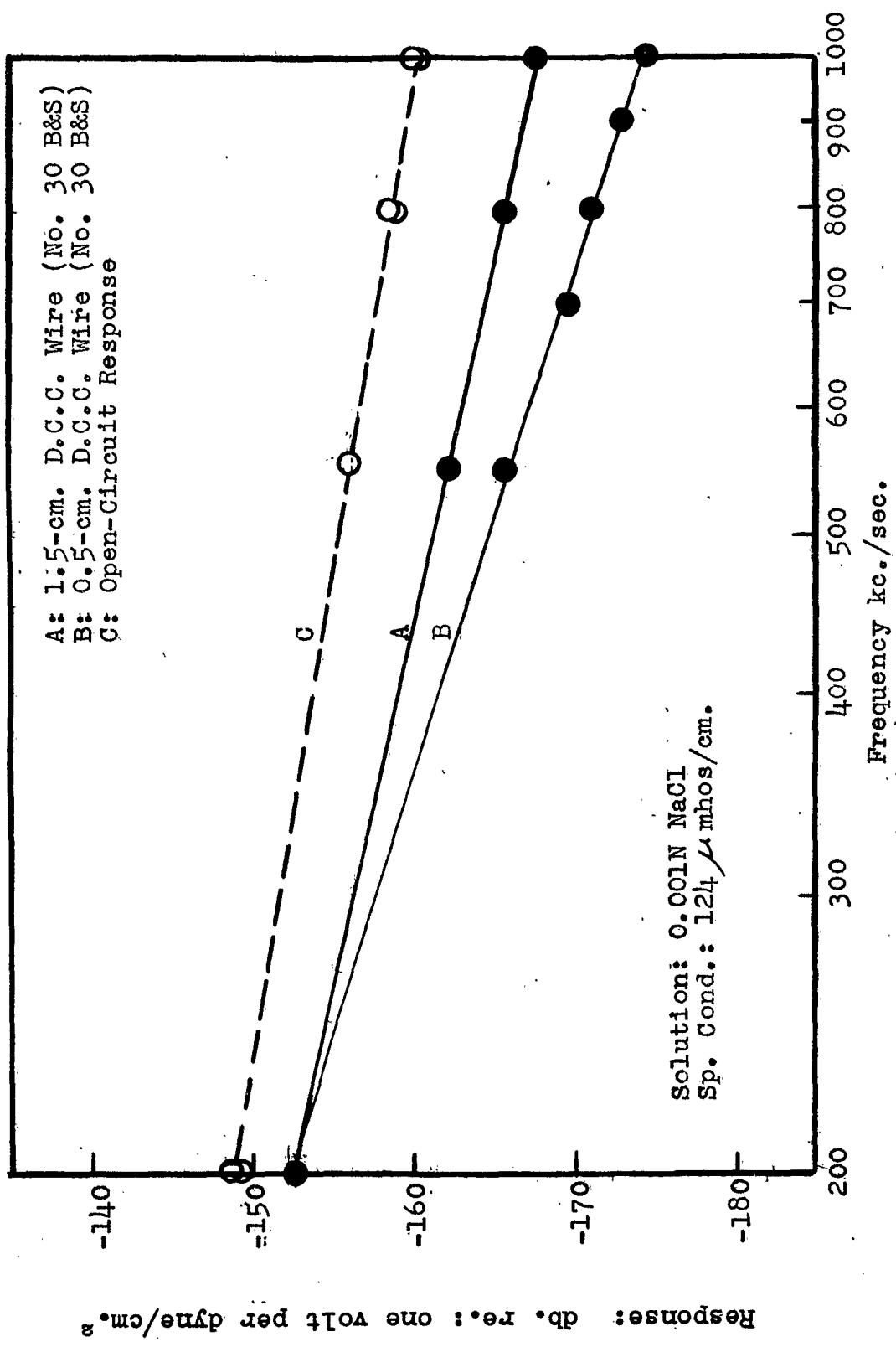


Figure 3: Dependence of Electrokinetic Effect on Frequency in 0.0001N NaCl.



A: 1.5-cm. D.C.C. Wire (No. 30 B&S)
B: 0.5-cm. D.C.C. Wire (No. 30 B&S)
C: Open-Circuit Response

Solution: 0.001N NaCl
Sp. Cond.: 124 μ mhos/cm.

Dependence of Electrokinetic Effect on Frequency
in 0.001N NaCl.

Figure 4₂

Response: db. re.: one volt per dyne/cm.²

frequency. The impedance values at 200 kc./sec. have been extrapolated from the values in the range 550 to 1000 kc./sec. This procedure was necessary because of the limited range of the impedance bridge. The reliability of such an extrapolation has been substantiated² in earlier work by measuring the effect with several different load impedances and solving simultaneous equations for the internal impedance associated with the electrokinetic effect.

The graphs in Figures 2-4 indicate that the response is a continuous function of frequency with no inflection points in the range 200 to 1000 kc./sec. This fact is of particular significance in hydrophone applications in that interpolation between frequencies is possible. With more conventional high frequency hydrophones, e.g., barium titanate, the non-uniform frequency response at frequencies above 100 kc./sec. requires a continuous frequency calibration. It is also evident from the data that the open-circuit response is independent of the wire length between the 0.5-cm. and 1.5-cm. lengths considered.

In Figure 5, the open-circuit response for the double, cotton-covered electrokinetic probes is plotted vs the logarithm of the frequency for several concentrations of sodium chloride. These data represent both the 0.5-cm. and 1.5-cm. probes since the open-circuit response for both are essentially the same. Figure 5 indicates that the open-circuit response in db. for all concentrations is a linear function of the logarithm of the frequency. It is evident, however, that the slope as well as the relative position is dependent upon the specific conductance.

The dependence of the electrokinetic effect on concentration for different frequencies is shown in Figure 6 for the 0.5-cm. cotton-covered copper wire and in Figure 7 for the 1.5-cm. probe. The data

TABLE 1

IMPEDANCE MEASUREMENTS FOR ELECTROKINETIC PROBES

Acous- tical Element	Specific Cond. of NaCl in μ mhos/cm.	Freq. in kc./ sec.	Load Impedance		Internal Impedance	
			Cap. Adm. in μ mhos	Parallel Cond. in μ mhos	Cap. Adm. in μ mhos	Parallel Cond. in μ mhos
0.5-cm. No. 30 D.C.C.	2.1	1000	242	12.3	31.4	6.7
		900	216	11.1	28.1	6.5
		800	189	10.2	25.1	6.1
		700	164	8.3	22.4	5.7
		550	126	6.7	17.6	4.9
		200	41.5	4.0	6.4	3.7
	17.5	1000	242	12.3	35.2	14.2
		900	216	11.1	30.5	14.1
		800	189	10.2	26.1	13.2
		700	164	8.5	22.4	12.7
		550	126	6.7	17.3	11.9
		200	41.5	4.0	6.1	10.0
	124	1000	242	12.3	47.1	55.5
		800	189	10.2	36.6	50.9
		550	126	6.7	24.5	45.0
200		41.5	4.0	8.9	37.0	
1.5-cm. No. 30 D.C.C.	2.1	1000	255	12.8	60.2	13.0
		800	198	10.5	49.3	11.2
		550	131	6.8	35.2	9.6
		200	45	3.9	13.0	6.8
	17.5	1000	255	12.8	65.9	28.0
		800	198	10.5	51.1	25.8
		550	131	6.8	35.2	23.4
		200	45	3.9	12.6	20.0
	124	1000	255	12.8	93.0	108
		800	198	10.5	73.0	94.3
		550	131	6.8	45.8	77.9
		200	45	3.9	15.1	57.9

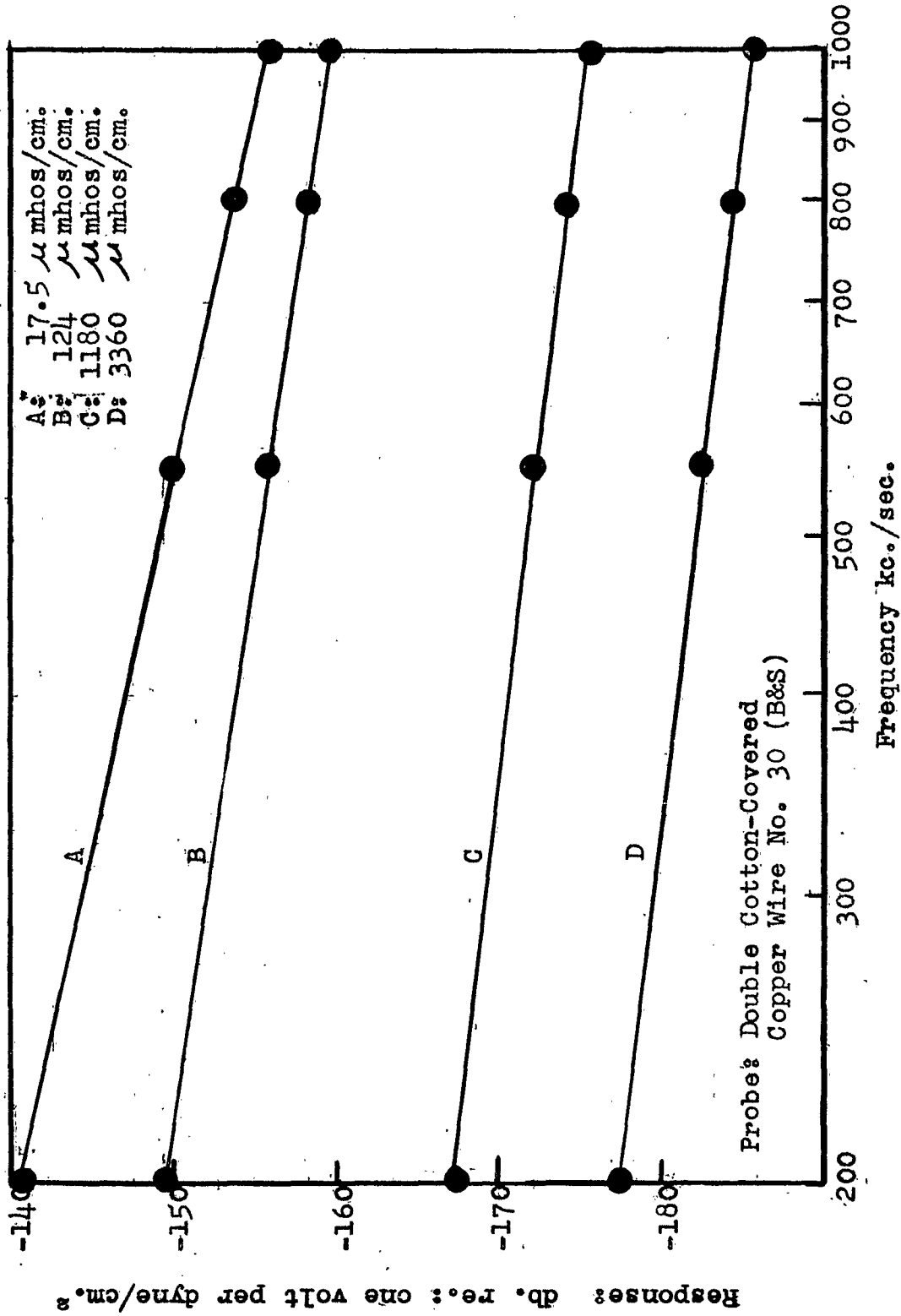


Figure 5: Dependence of Open Circuit Response of Electrokinetic Effect on Frequency in NaCl Solutions.

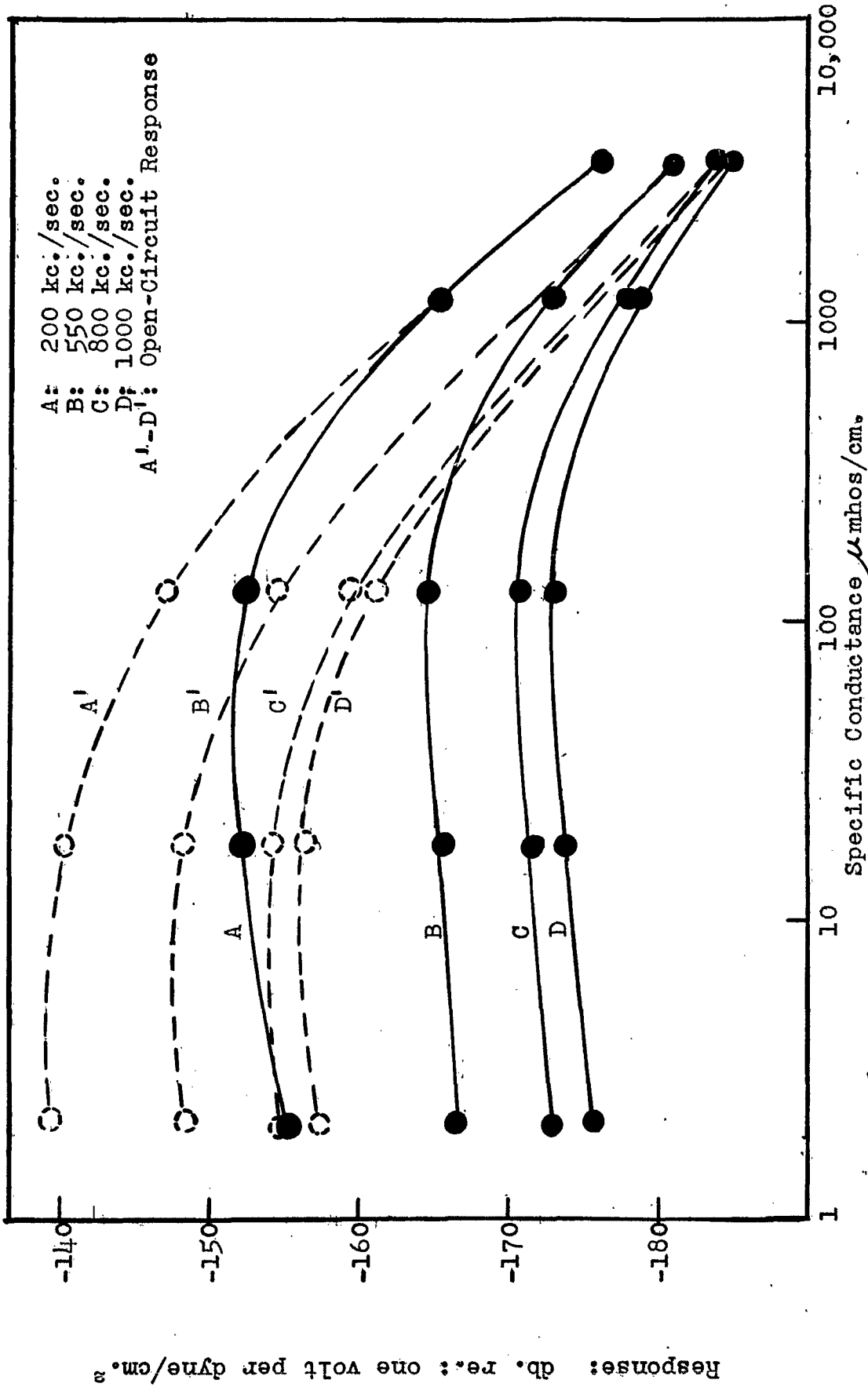


Figure 6:
Dependence of Electrokinetic Effect on Conductance
for a 0.5-cm. D.C.C. Wire in NaCl Solution.

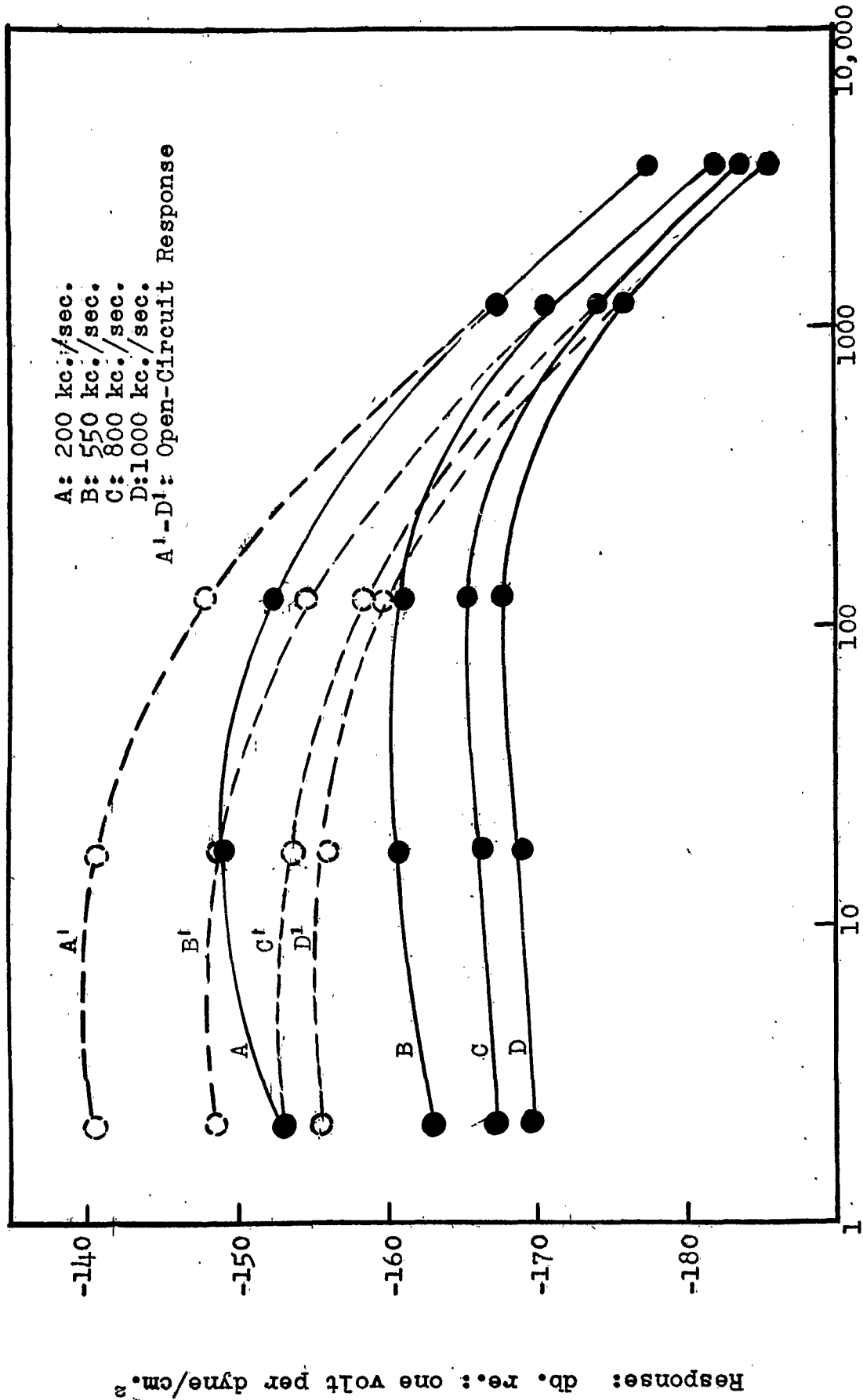


Figure 7: Dependence of Electrokinetic Effect on Conductance for a 1.5-cm. D.C.C. Wire in NaCl Solution.

are presented with the solid lines representing the terminated response and the dotted lines the calculated open-circuit response for each frequency.

A comparison of Figures 6 and 7 indicates that both the 0.5-cm. and 1.5-cm. length probes exhibit the same characteristics in their response. This is perhaps more clearly illustrated in Figure 8 in which the responses of a 0.5-cm. and 1.5-cm. probe at 200 kc./sec. are compared. The open-circuit responses for the two probes lie essentially on the same line. Similar plots can be made for all frequencies considered and, within experimental error, all the open-circuit voltages for the two probes under similar conditions are the same. The effect is seen to decrease with increasing concentration of electrolyte as would be expected on the basis of the decrease in d.c. streaming potential with increasing concentration.

In solutions with a specific conductance of $100 \mu\text{mhos/cm.}$ or greater, there is an approximately linear relationship between the conductance and open-circuit response as shown in Figures 6-8. With more dilute solutions, the ions associated with the solvent become significant, and therefore, the system is not the same as considered for the more concentrated solution.

In Figure 9, the frequency response of a 0.5-cm. double, silk-covered wire (No. 30, B&S) is compared with a cotton-covered probe of the same dimensions. The impedance measurements associated with this probe are presented in Table 2. The responses of the two probes appear to be on parallel lines, and therefore, have the same slope. This suggests that the frequency dependence of various probes with different coverings may be predicted from one calibration at a given frequency.

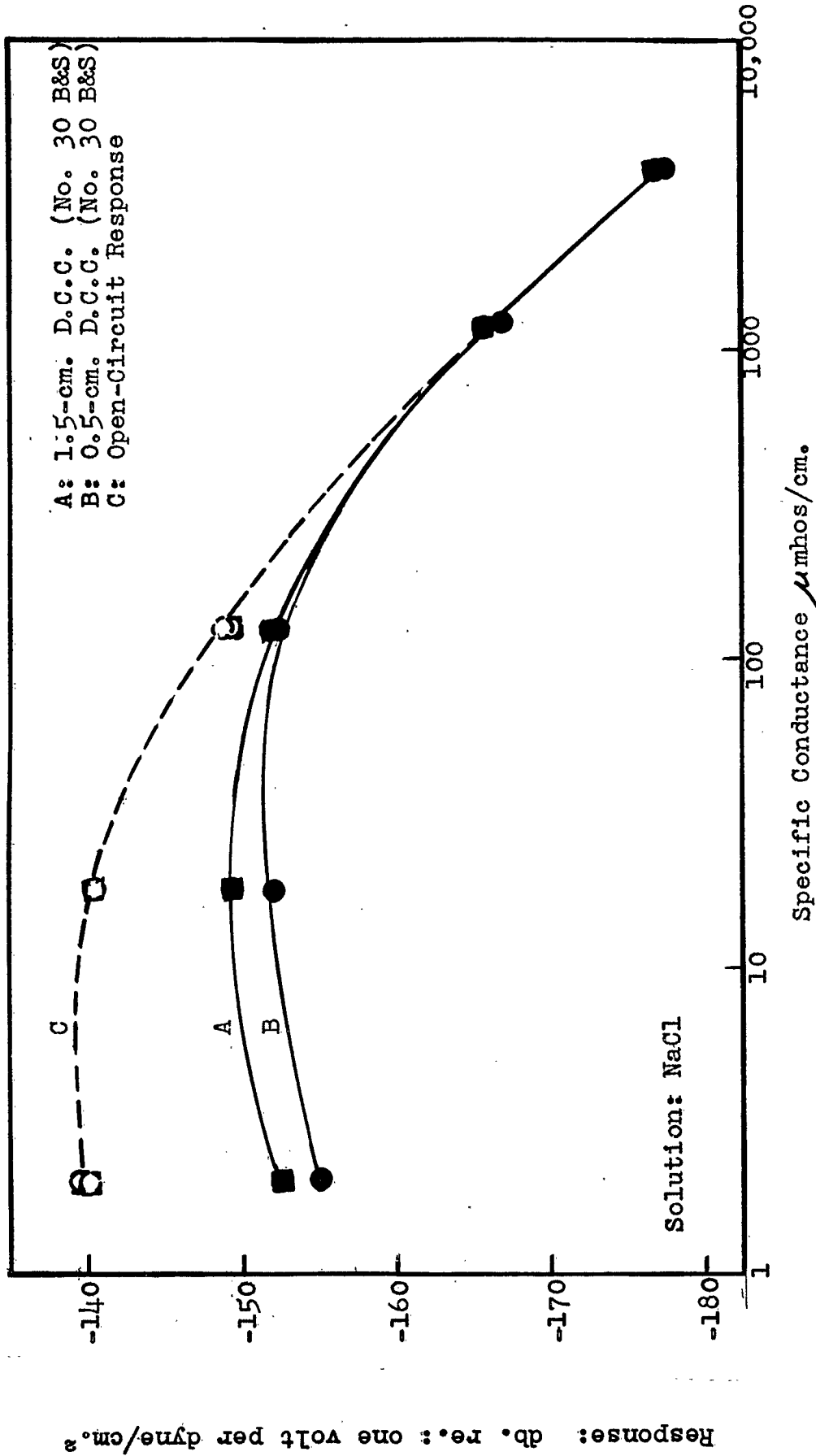


Figure 8: Dependence of Electrokinetic Effect on Conductance and Wire Length at 200 kc./sec.

TABLE 2
 IMPEDANCE MEASUREMENTS FOR DOUBLE, SILK-COVERED
 ELECTROKINETIC PROBE

Frequency in kc./sec.	Load Impedance		Internal Impedance	
	Capacitive Admittance in μ mhos	Parallel Cond. in μ mhos	Capacitive Admittance in μ mhos	Parallel Cond. in μ mhos
1000	223	10.7	31	9.9
700	155	9.6	23	9.6
550	120	6.4	17	9.4
200	34	4.5	11	9.0

Probe: 0.5-cm. No. 30 D.S.C. Copper Wire
 Solution: NaCl, Specific Conductance 20.8 μ mhos/cm.

TABLE 3
 DEPENDENCE OF FREQUENCY RESPONSE OF ELECTROKINETIC
 EFFECT ON WIRE SIZE IN 0.0001 N SODIUM CHLORIDE

Acoustical Element	Frequency in kc./sec.	Acoustical Response in db. re.: one volt per dyne/cm.	
		Terminated	Open-Circuit
No. 26(B&S) 0.5-cm. D.C.C.	1000	-176.1	-159.0
	800	-173.6	-155.6
	550	-169.0	-152.9
	200	-154.1	-141.7
No. 30(B&S) 0.50cm. D.C.C.	1000	-174.6	-157.0
	800	-172.6	-155.9
	550	-167.5	-151.3
	200	-152.4	-140.9
No. 34(B&S) 0.5-cm. D.C.C.	1000	-175.0	-158.3
	800	-173.1	-157.1
	550	-167.8	-153.7
	200	-153.1	-142.6

Specific Conductance: 15.8 μ mhos/cm.

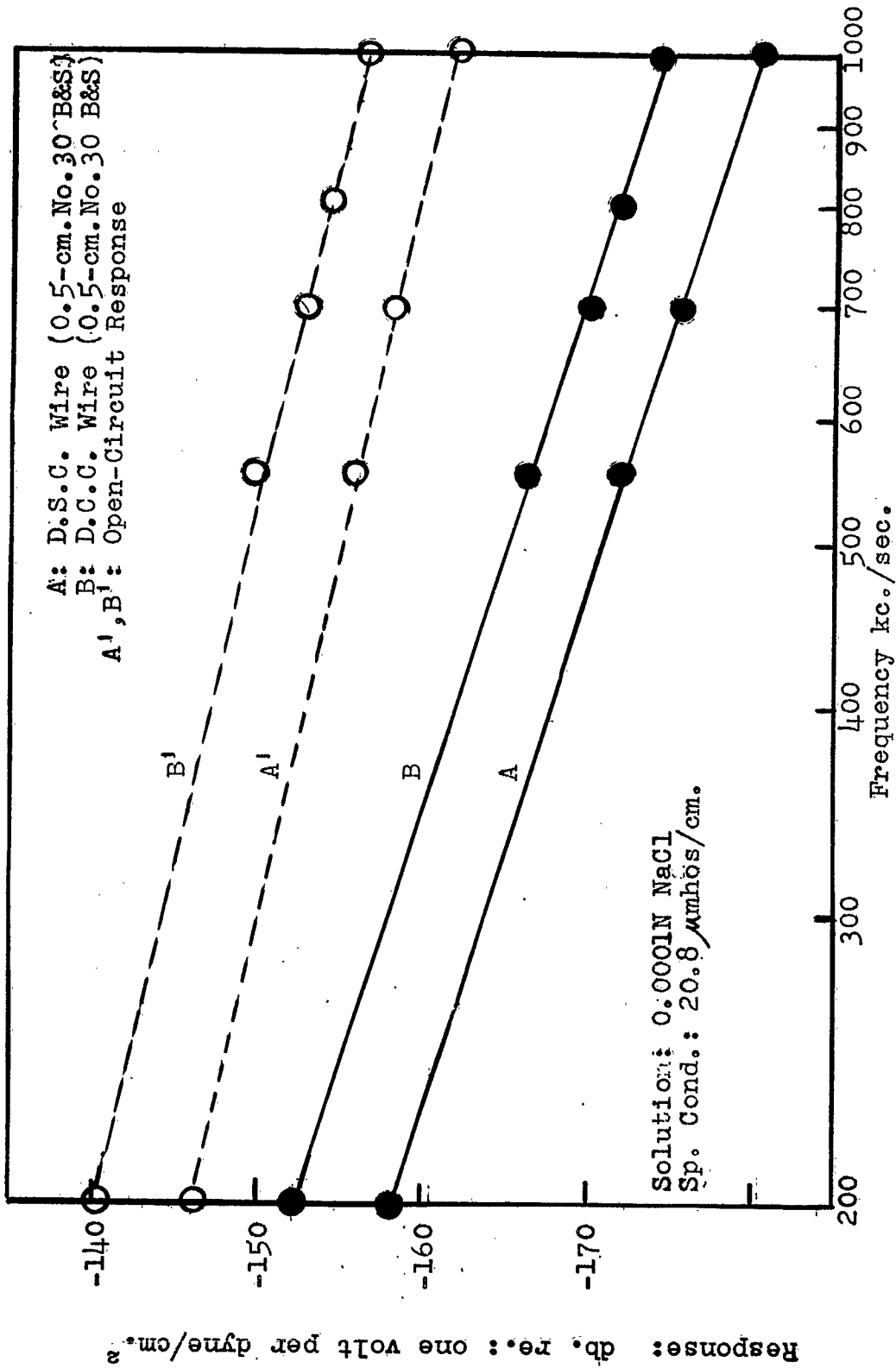


Figure 9:
Dependence of Electrokinetic Effect on
Frequency for Cotton and Silk Covered Wire.

The data for the frequency dependence of a 0.5-cm. double, cotton-covered probe on wire size are given in Table 3. The exposed elements were No. 26, 20 and 34 (B&S) double, cotton-covered copper wire. The data are presented in terms of terminated response as well as the calculated open-circuit voltage. There seems to be no significant dependence on wire size within the limited range considered here. The three wire sizes investigated have approximately the same characteristics in their frequency dependence for both the terminated and open-circuit response. The slight variations in Table 3 may be associated primarily with differences in the cotton coverings rather than the wire diameter.

3. Interpretation and Conclusions

The following conclusions may be reached concerning the characteristics of the electrokinetic effect in the frequency range 200 to 1000 kc./sec. on the basis of the present work.

- (1) The response is a continuous function of frequency and does not show any of the peaks and inflection points usually characteristic of acoustical probes for work at frequencies above 100 kc./sec.
- (2) The open-circuit response associated with the effect is substantially independent of probe length and dependent on wire gage only to a minor extent provided the diameter is relatively small compared to the wavelength.
- (3) The frequency dependence of the response for probes involving silk and cotton coverings is essentially the same.
- (4) The amplitude of the effect is approximately directly proportional to the displacement amplitude for solutions of low specific conductance (< 25 micromhos/cm.) Thus the response expressed in terms of pressure amplitude is inversely proportional to the frequency. With increasing conductance, the response in terms of pressure amplitude approaches a 0.6 power dependence on frequency.

These conclusions are significant in regard to the use of this effect as a high frequency probe. The linear relationship between the response

in db. and frequency would eliminate the necessity of calibration at a large number of frequencies since measurements at only two frequencies would indicate the frequency response over a reasonably large range.

One mechanism, presented previously², is illustrated in Figure 10. The black dots surrounding the central wire represent somewhat idealistically

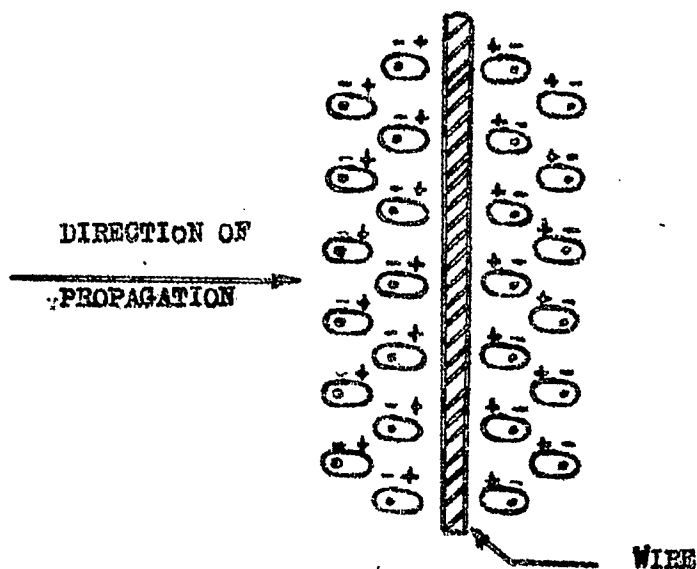


Figure 10: Mechanism involved with Electrokinetic Probe

the cross section of the fibers in a plane parallel to the direction of propagation. In the presence of ultrasonic waves, the diffuse layer of ions surrounding each fiber becomes periodically asymmetric in the direction of propagation. A difference in the displacement of the ions of the diffuse layer and the fibers is to be expected in terms of their physical characteristics. Figure 10 represents the situation when a displacement node is instantaneously at the position of the central wire. Since the predominant charge of the diffuse layer of ions is opposite to that of the fiber, there should be a periodic potential difference between the central wire and the solution outside the fiber covering. The solution in contact with the wire

in the plane perpendicular to the direction of propagation and the axis of the wire loads the a.c. effect internally, and hence reduces the magnitude in a sense.*

An attempt is being made to interpret the model in Figure 10 in a quantitative fashion. Unfortunately, the problem is quite complex at frequencies of the order of 10^6 sec.^{-1} . The approximate dependence of the effect on electrochemical parameters can be deduced in terms of the close analogy between the mechanism in Figure 10 and that associated with colloidal vibration potentials^{11,13}. For the case where the dimensions of the colloidal particles are large compared to the effective thickness of the diffuse layer of ions surrounding the particles, Enderby¹⁴ has developed the following equation for the amplitude of the potentials:

$$\Phi_0 = (\bar{n}_k w_k f c \xi \alpha / k T \eta \kappa^2) a_0 \quad (1)$$

where

$$a = \kappa^2 / [\kappa^4 + (\omega f / k T)^2]^{1/2} \quad (2)$$

a_0 is the velocity amplitude, c the velocity of sound in the medium, η the viscosity of the solvent, ω the angular frequency, k the Boltzman constant, T the absolute temperature, \bar{n}_k the number of colloidal particles per cm^3 , w_k the apparent mass of each particle, f the frictional

* An alternate interpretation is to consider the coverings as the equivalent of a large number of poorly defined capillaries. Either interpretation represents a marked over simplification.

13. Yeager, Dietrick, and Hoyerka, J. Acoust. Soc. Am., 25, 456 (1953).

14. J. Enderby, Proc. Roy. Soc. (London), 207A, 329 (1951).

coefficient of the cations and the anions (assumed to be the same, ϵ) the zeta potential, and K the effective thickness of the diffuse ionic layer. The latter is related to the specific conductance (κ) by the approximate

$$\kappa^2 = 4\pi f K / D k T. \quad (3)$$

For specific conductances of 10^{-4} mhos/cm. or greater and angular frequencies of 10^7 or less, the term ϵ is very close to unity. Equation (1) then reduces

$$\Phi_0 = B \left(\frac{D \epsilon}{\eta K} \right) c a_0 \cong B' \left(\frac{D \epsilon}{\eta K} \right) p_0 \quad (4)$$

where B is a function of the apparent colloid concentration and the mobility of the electrolyte. The term p_0 is the pressure amplitude of the ultrasonic waves and $B' = B/\rho$ where ρ is the density of the medium. In the case of the electrokinetic effect, the same equation should be applicable except that B is a function of the fiber geometry and the frequency. The dependence of the electrokinetic effect on the ratio of zeta potential to specific conductance is evident from eq. (4).

The general equation for d.c. streaming potentials is

$$E = \frac{D \epsilon}{4\pi \eta K} p \quad (5)$$

where p is the pressure driving the solution through the porous plug or capillary. The marked similarity between eq. (4) and eq. (5) has been demonstrated experimentally in terms of the excellent correlation of the a.c. electrokinetic effect at ultrasonic frequencies with d.c. streaming potential data for the same fibers.

I THE FREQUENCY DEPENDENCE AND RELATED CHARACTERISTICS OF THE A.C. POLARIZED GAS ELECTRODE EFFECT

On the basis of previous work with the polarized hydrogen electrode, it has been concluded that this effect can be primarily attributed to the modulation of the I-R drop in the solution adjacent to the electrode surface by periodically expanding and contracting gas bubbles. Although this hypothesis is reasonably well established, the present investigation has been directed towards further substantiating this conclusion and at the same time establishing the frequency characteristics for the polarized hydrogen electrode.

1. Experimental Techniques:

The acoustical system used in this work was similar to that employed for investigating the electrokinetic effect except for the probes involved in the detection of the effects. A description of the acoustical system is presented in the appendix to this report.

A diagram of the electrode used for detecting this effect is given in Figure 11. The hydrogen gas was liberated by electrolysis on a cathode consisting of a platinum wire, (No. 39, B. & S.) sealed in soft glass tubing. The length of the exposed wire was approximately 0.3 cm. and the calculated apparent area 0.25 cm.^2 . The surface of the wire was platinized. The lead wire from the cathode was shielded by a brass probe housing which connected to the pre-amplifier housing through a single-contact microphone connector. The a.c. potentials were measured between the platinized-platinum cathode and the bulk of the solution or ground.

A platinum wire sealed in soft glass tubing served as the anode

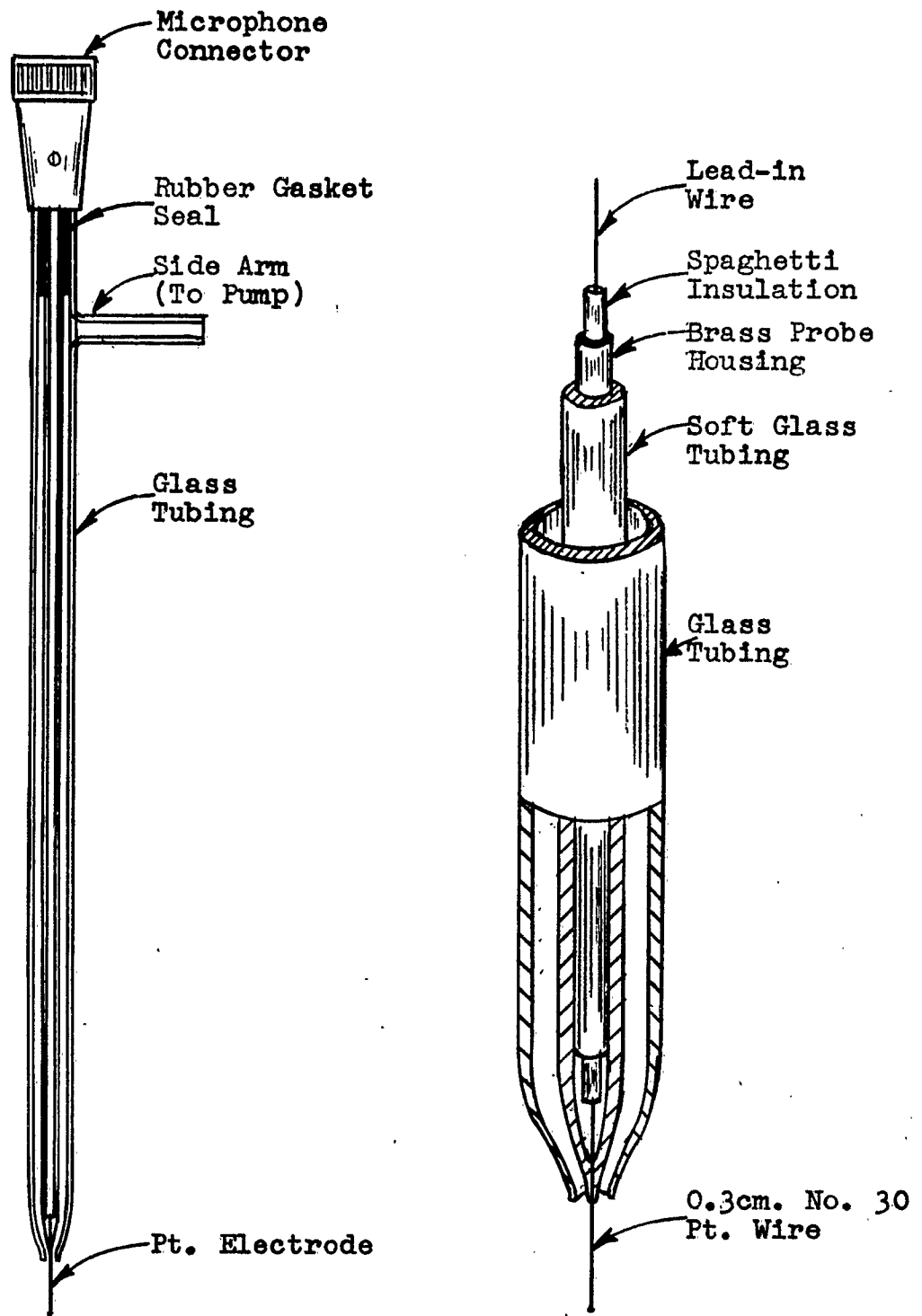


Figure 11: Acoustical Hydrogen Electrode

with approximately 4 cm. exposed to the solution. The anode was isolated from the solution around the cathode by a fritted-glass disc to minimize contamination by oxygen gas. The anode was not in the ultrasonic field, and did not contribute directly to the a.c. potentials.

The polarizing current was obtained from two voltage-regulated power supplies, placed in series to provide a total voltage of 500 volts at a maximum of 100 ma. The polarizing current was measured with a Simpson milliammeter, Model 373. Since the alternating components were developed on the cathode relative to ground, a two-section, radio-frequency filter was used in the lead wire from the source of the polarizing current to the cathode. This filter prevented the d.c. source of polarizing current from loading the polarized electrode with respect to the acoustically produced radio-frequency component in the electrode potential.

Considerable difficulty was encountered when this effect was investigated at 1 mc./sec. The bubble cloud which formed about the electrode attenuated and scattered the ultrasonic waves to a far greater extent than at 200 kc./sec. A steady a.c. response could not be obtained. On the basis of theoretical considerations it is evident that the bubbles immediately adjacent to the surface are responsible primarily for the effect and that the bubbles at any appreciable distance contribute virtually nothing to the observed effect. This suggested the use of a high velocity directed flow of solution passed the electrode to remove the latter type of bubbles, i.e., the bubble cloud. Such a flow of electrolyte would have only a minor effect on

the bubbles at the surface.

The details of the construction used to accomplish this purpose are shown in Figure 11. A glass tube drawn to a large capillary tip has been placed over the tube containing the platinum electrode with sufficient space between them for the flow of the solution. The glass envelope has a side arm at the top through which the electrolyte is pumped by a high velocity centrifugal pump from the acoustical cell and cycled through the system. This technique proved to be very satisfactory in removing the gas bubbles, and hence, allowed the ultrasonic waves to interact with the gas bubbles on the electrode surface. With this type of cathode, the fluctuations in the acoustical response have been reduced to less than 5% at 1 mc./sec. with current densities as high as 500 ma./cm.²

In most of the measurements to be described, the a.c. polarized hydrogen electrode has been studied in sodium sulfate solutions with the concentrations determined from specific conductance measurements. The solutions have been saturated with purified hydrogen gas prior to the acoustical measurements.

2. Experimental Results:

In Figure 12 is shown the frequency dependence of the acoustical response in sodium sulfate solutions with a specific conductance of 49 micromhos/cm. and a polarizing current density of 240 ma./cm.² The solid line represents the terminated response in db.re: 1 volt per dyne/cm². The dotted line indicates the open-circuit values calculated from impedance measurements associated with the electrode assembly as described for the electrokinetic effect. For the hydrogen electrode

effect the situation was more complex. The internal impedance has been determined with the unpolarized probe* in contact with the solution with no bubbles present. The calculated open-circuit response indicates that the loading effect is appreciable in the dilute solutions. In solutions with specific conductance greater than 100 micromhos/cm., the terminated response is approximately the same as the open-circuit response. Figure 12 indicates that the effect is a continuous function of the frequency with no apparent inflection points. The relative frequency dependence of this effect is a function of the conductivity of the solution and the polarizing current density.

In Figure 13 is presented the dependence of the observed response on frequency in sodium sulfate solution with specific conductances of 215 and 400 micromhos/cm. at a polarizing current density of 80 ma./cm.²

The dependence of the a.c. hydrogen electrode effect on conductance of a sodium sulfate solution for several frequencies is illustrated in Figure 14. These data are presented for the frequencies 200, 550, and 1000 kc./sec. with a polarizing current density of 200 ma./cm.² The loading effect on the response in the dilute solutions is apparent by comparison of the calculated open-circuit response (dotted lines) with the terminated response (solid lines) in Figure 14. In the more concentrated solutions, the effect tends to have a constant frequency dependence with increasing concentration.

In Figure 15 the dependence of the a.c. hydrogen electrode effect is

* Since the effect is produced when bubbles are formed, the impedance may differ to a small extent with the gas bubbles surrounding the electrode. Further impedance measurements will be made with polarized electrodes.

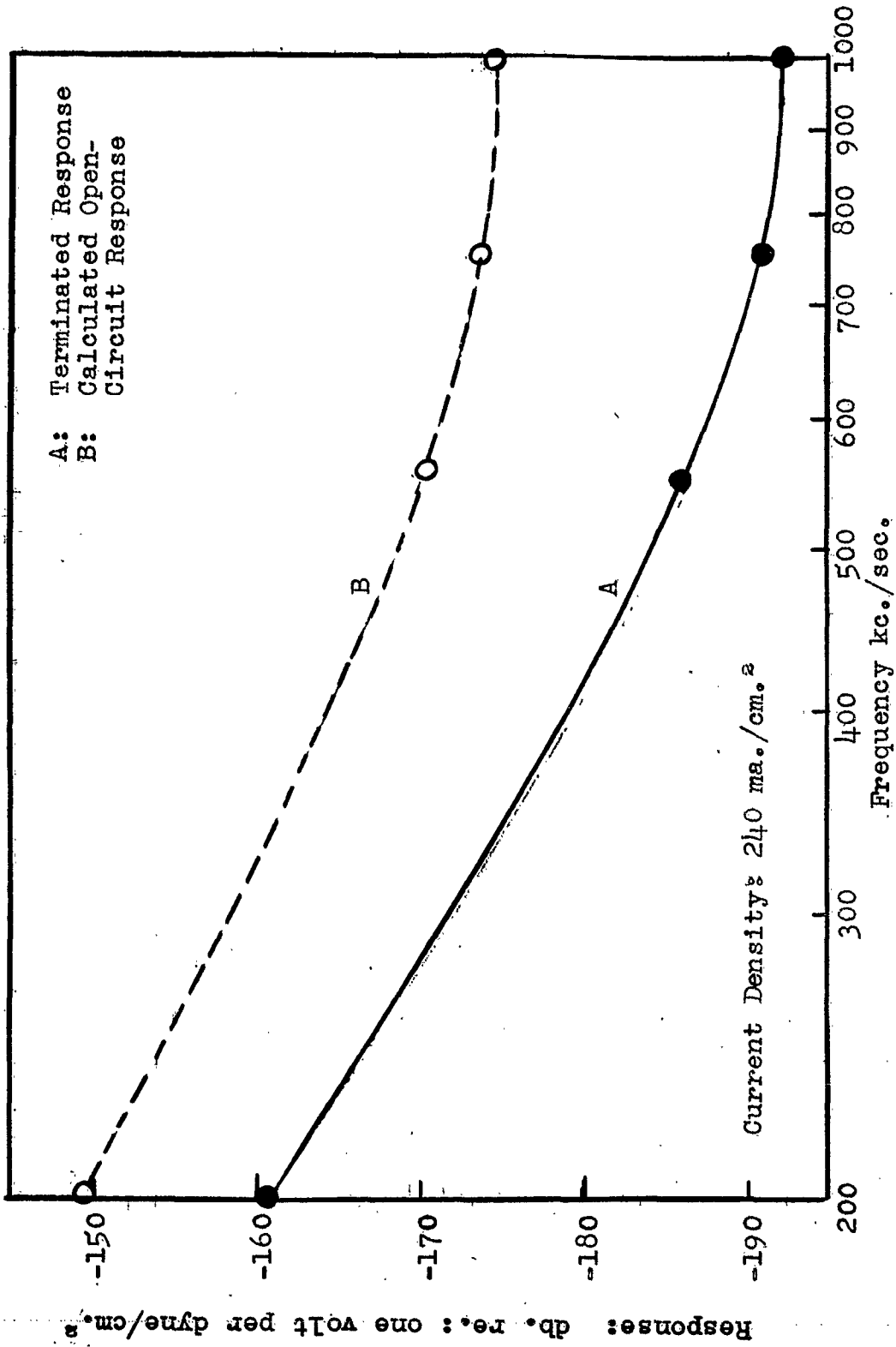


Figure 12: Dependence of A.C. Hydrogen Electrode Effect on Frequency in 0.0001M Na₂SO₄.

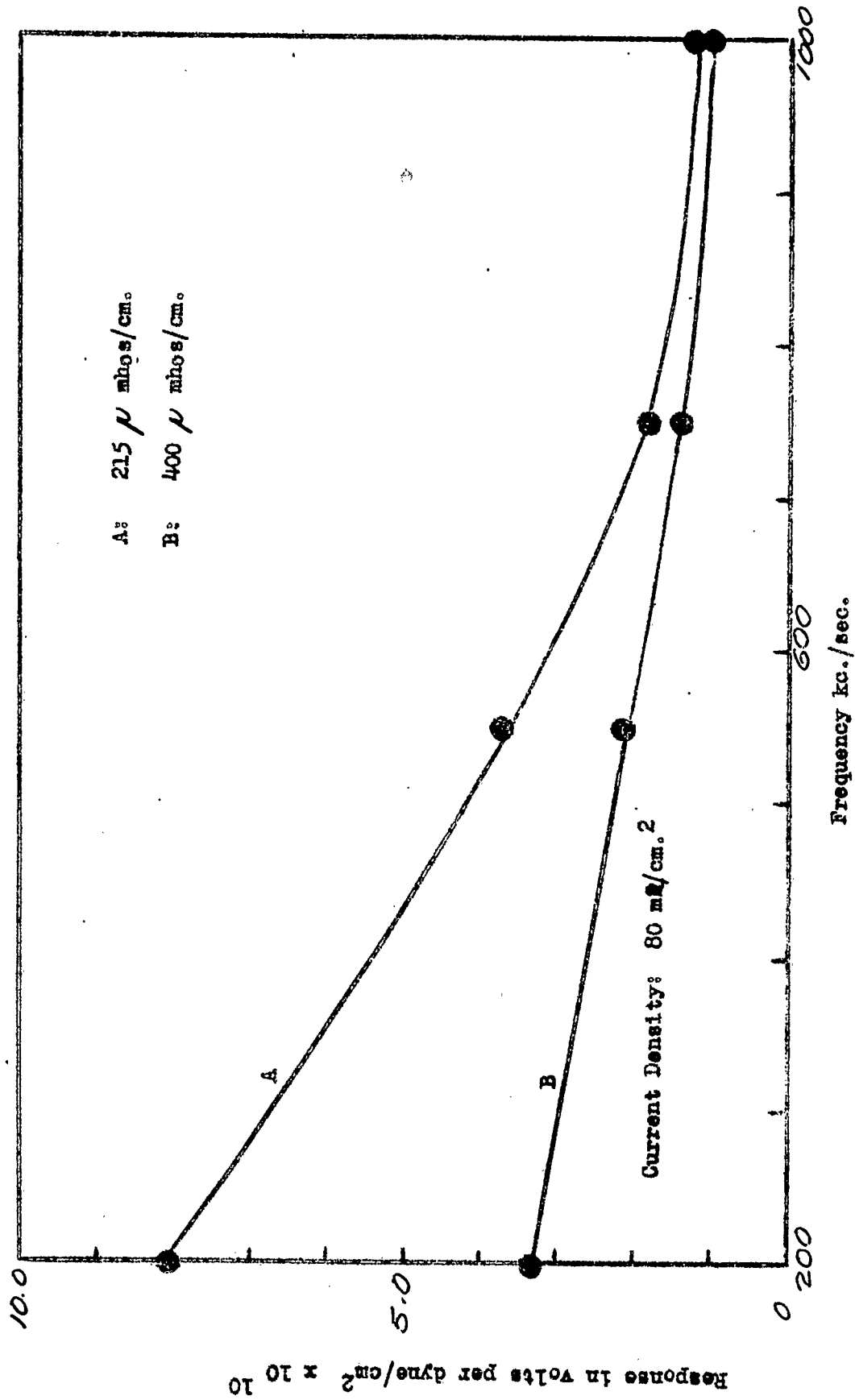


Figure 13: Frequency Dependence of the A.C. Polarized Gas Electrode Effect.

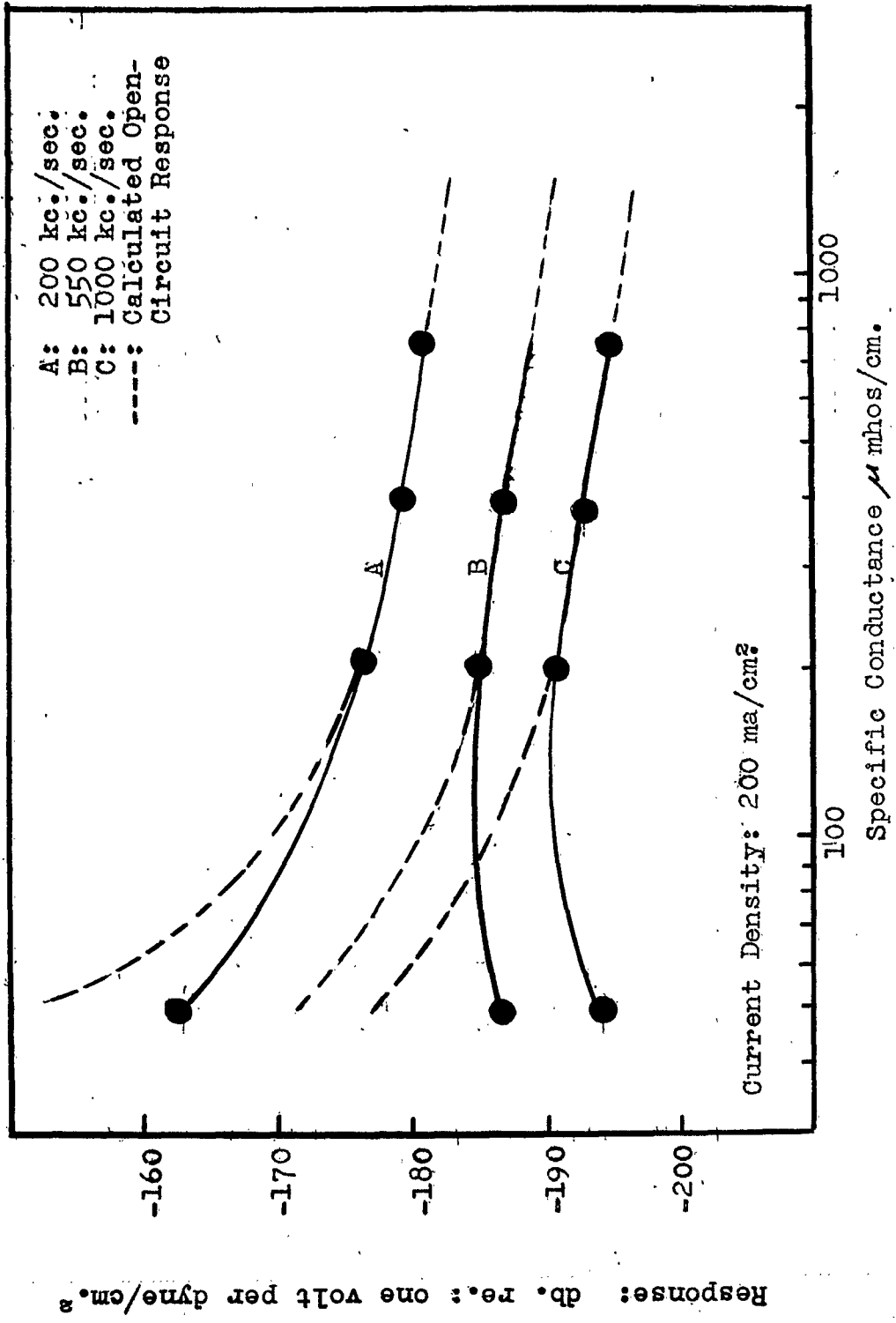


Figure 14: Dependence of A.C. Hydrogen Electrode Effect on Conductance in Na₂SO₄ Solutions.

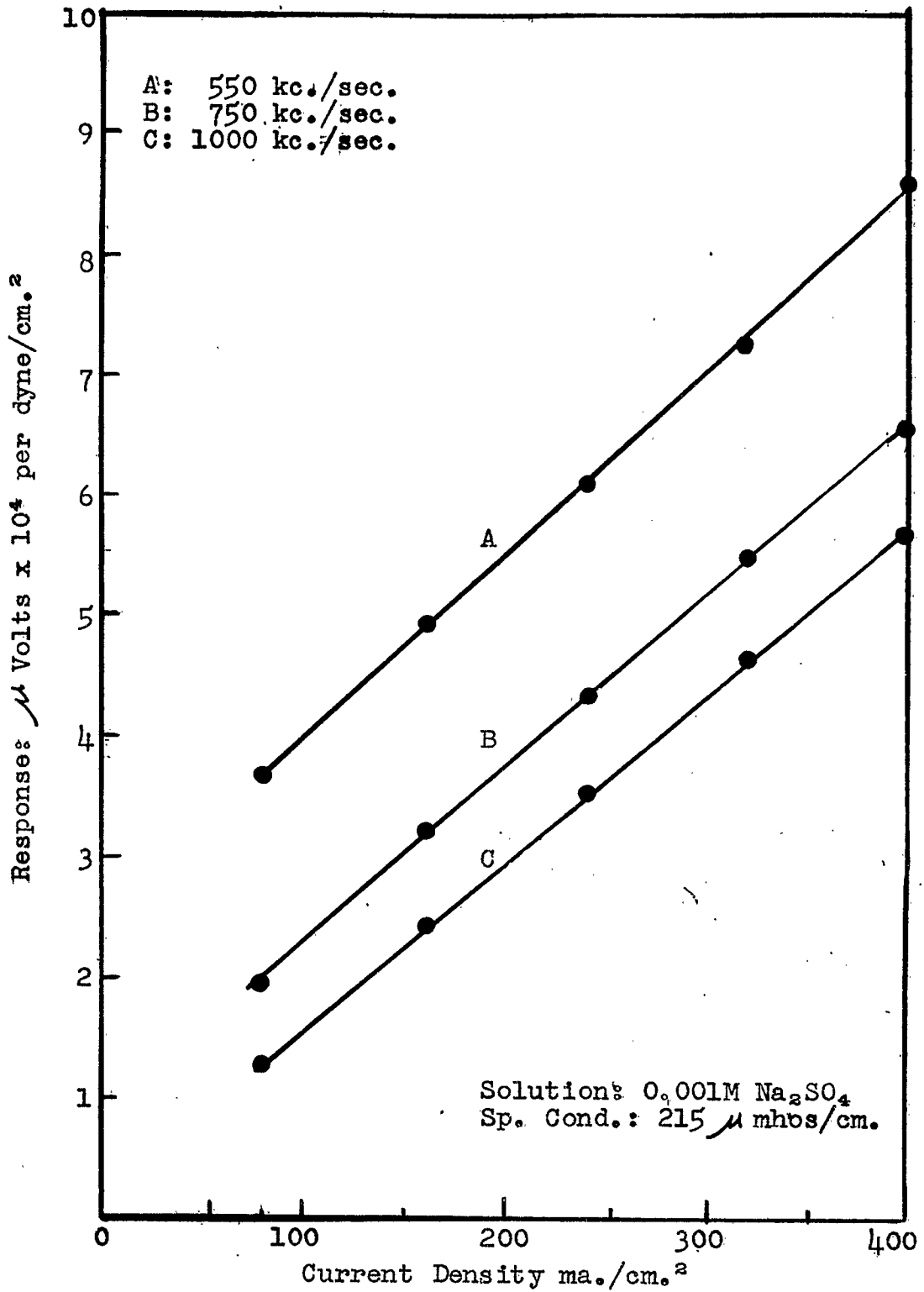


Figure 15: Dependence of A.C. Hydrogen Electrode Effect on Current Density.

considered as a function of the polarizing current density in sodium sulfate solution with a specific conductance of 215μ mhos/cm. For the frequencies and current density range considered here, the effect is linearly dependent on the current density. Similar dependence is noted for 200 kc./sec. in Figure 16. This is in contrast to the non-linearity noted in previous work without the directed flow of electrolyte.

The magnitude of the effect has also been determined as of a function of the acoustical amplitude. Within the limits of the intensity available, the effect is linearly dependent upon the acoustical pressure. In Figure 17 is shown the response of the hydrogen electrode effect at 200 kc./sec. with increasing acoustical amplitude of the ultrasonic waves. The response is recorded in microvolts and the acoustical pressure amplitude in atm. as measured with a calibrated barium titanate hydrophone. A similar linear dependence on acoustical amplitude has been found for the other frequencies considered. This is in contrast to that found in the previous work at 200 kc./sec. where a complex dependence was observed. The complex dependence can be attributed to the interaction of the ultrasonic waves with the gas bubbles in the vicinity of the electrode under static solution conditions.

Since the acoustical response of the polarized hydrogen electrode presented here has been obtained with a d.c. stream of electrolyte to remove the bubbles, the dependence on this stirring action has been considered. The response was very unstable under static solution conditions at the higher frequencies; therefore, the study of stirring effects has been carried out at 200 kc./sec. In Figure 18 is shown the dependence on stirring at 200 kc./sec. in a sodium sulfate solution with a specific conductance of 790μ mhos/cm. The lower curve repre-

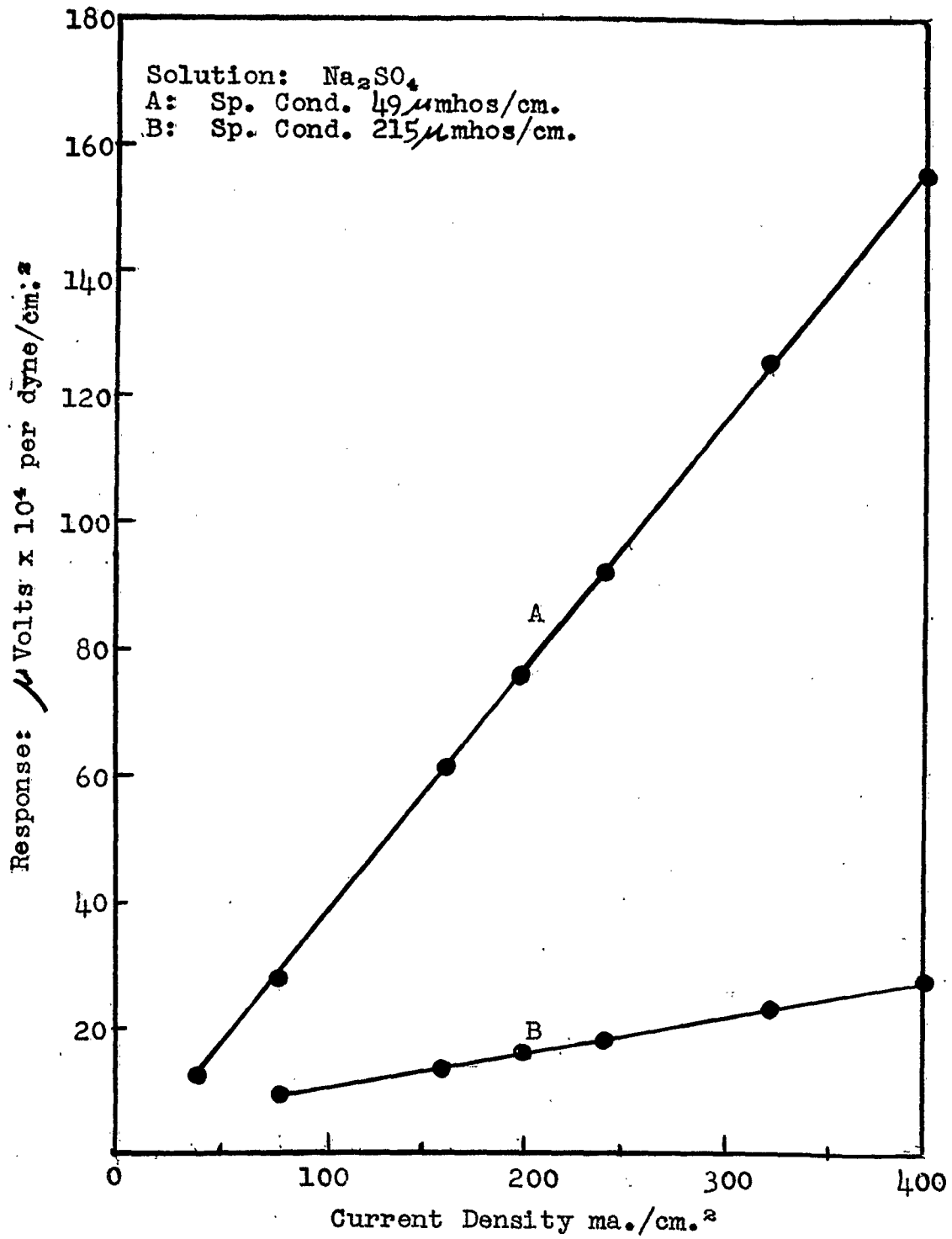


Figure 16:

Dependence of A.C. Hydrogen Electrode Effect on Current Density at 200 kc./sec.

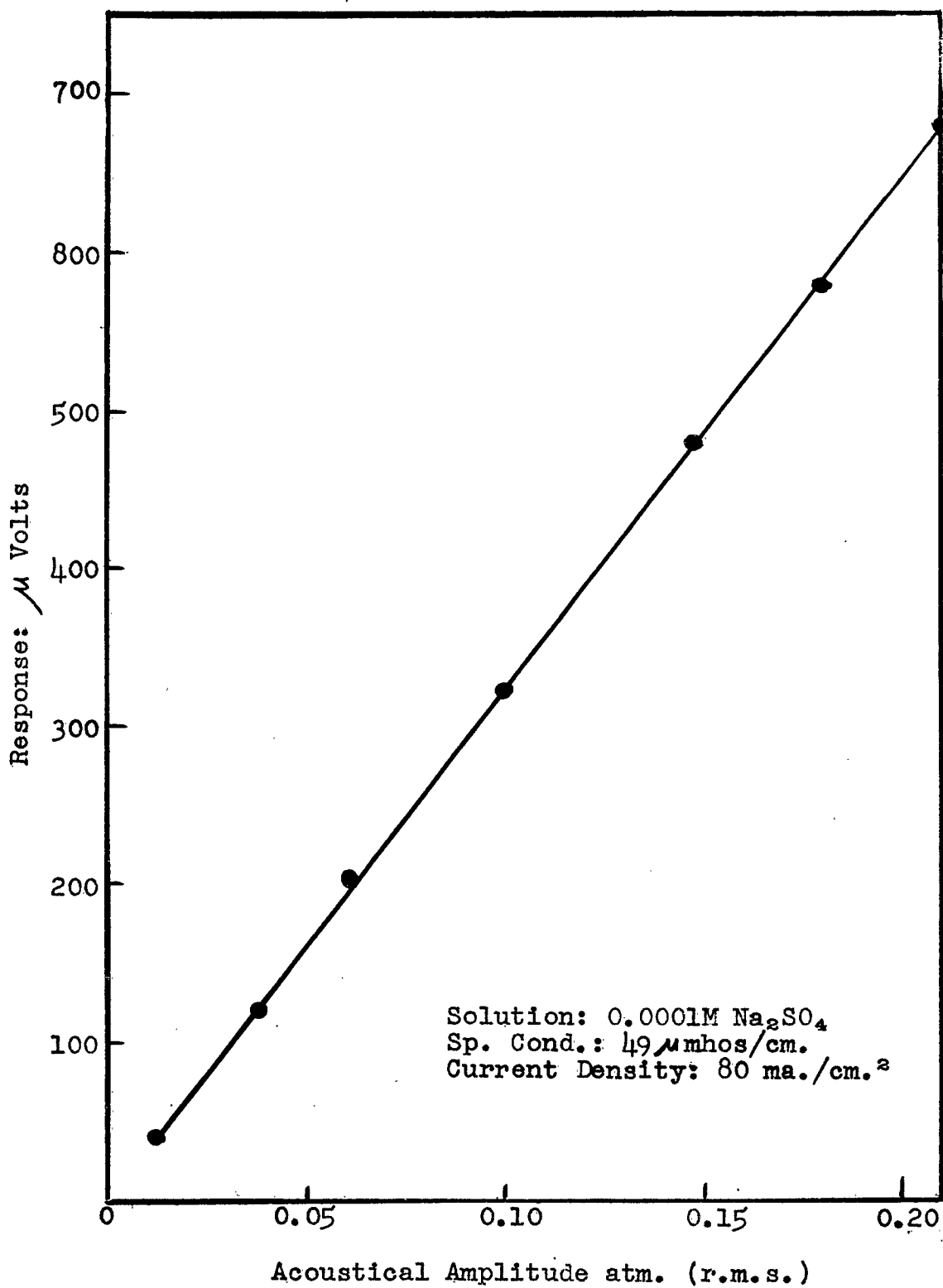


Figure 17a
Dependence of A.C. Hydrogen Electrode Effect on Acoustical Amplitude at 200 kc./sec.

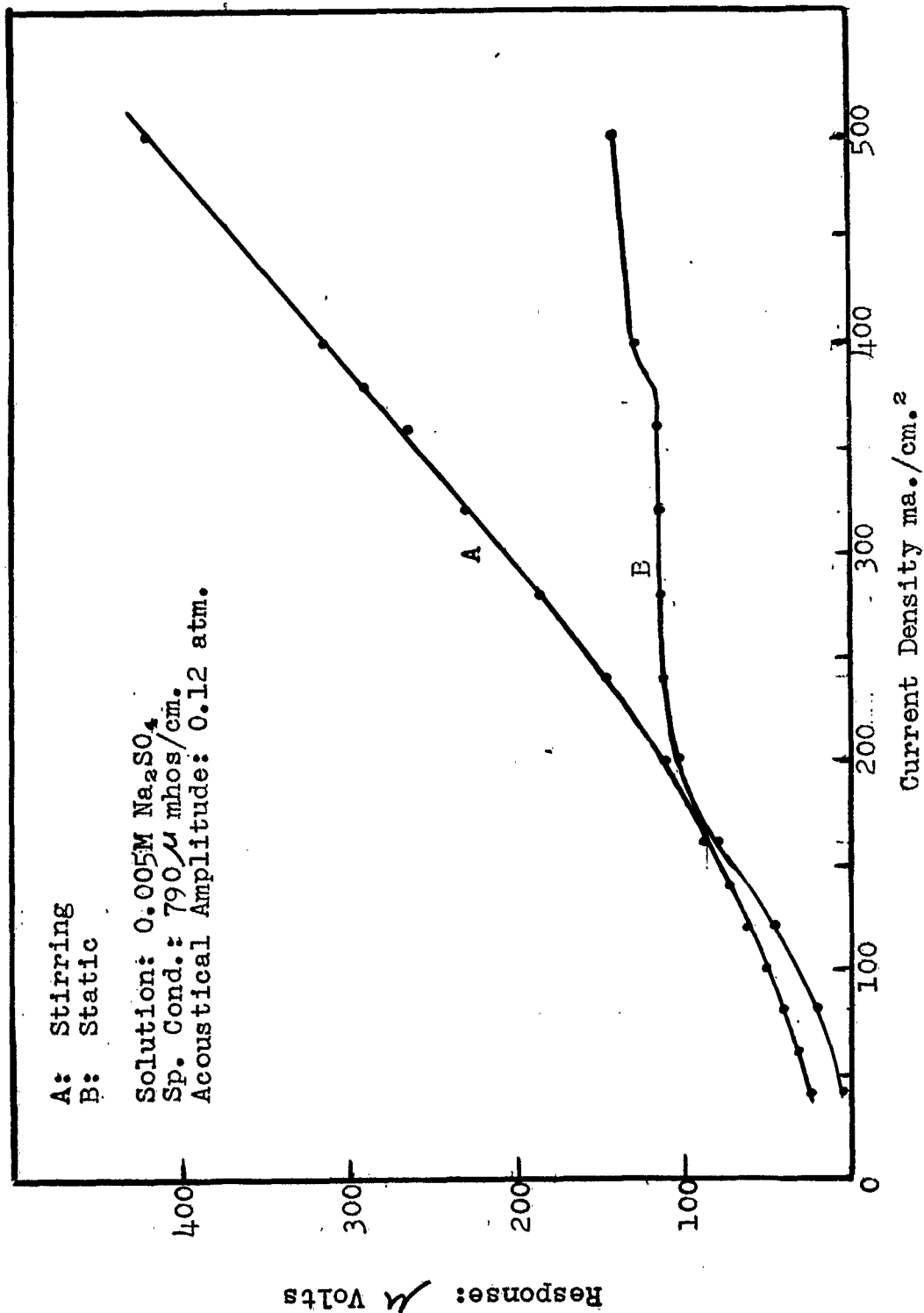


Figure 18: Dependence of A.C. Hydrogen Electrode Effect on Stirring and Current Density at 200 kc./sec.

sents the response under static solution conditions with the gas bubbles allowed to diffuse into the solution around the electrode. The characteristic plateaus are present as described in the previous work at 200 kc./sec. The upper curve is the response when the electrolyte is flowing past the cathode surface to remove the gas bubbles. It is evident that the magnitude of the effect is increased as the plateaus are eliminated. The complex dependence in the absence of directional flow is associated with the gas bubbles present in the vicinity of the electrode. These bubbles attenuate and scatter the sound waves in a complex fashion.

The following experiment was devised to confirm the conclusion that the modulation of the I-R drop in the immediate vicinity of the electrode produced the acoustical response. The polarizing current was interrupted while the polarized hydrogen electrode was exposed to the ultrasonic waves. According to the hypothesis advanced above, the effect should vanish virtually instantaneously.

The apparatus used for interrupting the polarizing current consisted of a gating tube inserted in the polarizing circuit. The tube was biased to operate at saturation current with no signal on the grid. A negative pulse was placed on the grid sufficient to cut the tube off at a time when the ultrasonic pulse was producing the a.c. effect. When the gating tube was cut off by the negative pulse, the polarizing current was also cut off and the resulting acoustical response observed on the oscilloscope. A suitable filter network has been inserted in the input circuit to the pre-amplifier to prevent the amplifiers of the detection apparatus from being blocked by the d. c. pulse.

The results of the above experiment indicate that the acoustical

response is terminate within the resolving time of the filter network and the amplifiers when the current is cut off, i.e., 0.001 sec. There is relatively little doubt that the effect is produced by a modulation of the I-R drop in the immediate vicinity of the electrode surface as a result of the interaction of the ultrasonic waves with the bubbles at the surface.

In work with the hydrogen electrode effect involving continuous ultrasonic propagation, the problem of electromagnetic coupling can be eliminated by modulating the d.c. polarising current with an audio-frequency component. The detection apparatus can be tuned to the resulting side band frequency which is not present in the electromagnetic coupling. This technique has been used in our laboratory and has proved to be very satisfactory in this application.

3. Interpretation and Conclusions:

From the experimental results obtained in this investigation as well as the observations made in the previous work at 200 kc./sec., the hydrogen electrode effect may be attributed to the modulation of the I-R drop in the solution adjacent to the electrode. The acoustical response of the hydrogen electrode indicates that the gas bubbles at the electrode surface are most effective in producing the a.c. effect. The bubble cloud present around the electrode in the absence of a directional flow scatters the sound in a complex fashion, thereby reducing the observed effect.

The alternating components can be explained in terms of periodic variations in the dimensions of the gas bubbles at the electrode surface. The gas bubbles are formed by electrolysis at the electrode

surface by the discharge of the hydrogen ions to form hydrogen gas.

The surface of the electrode acquires a discontinuous film of gas bubbles which may be considered as a part of a variable resistance. The size and quantity of the gas bubbles will determine the effective impedance to the flow of ions. The effective area of the electrode surface may be considered as being decreased by the presence of the gas bubbles.

When sound waves are introduced into such a system, the gas bubbles undergo periodic contraction and expansion. Since the gas bubbles are periodically changing their dimensions, the effective impedance will vary in a similar fashion. The potential developed across this impedance as a result of the current flow will likewise be a periodic function of the same frequency as the acoustical waves.

The a.c. component in the electrode potential may be represented by an equation of the form

$$\Phi = I (Z_s^o) \exp i\omega t \quad (6)$$

where Φ is the alternating component, I the polarizing current, (Z_s^o) the amplitude of the impedance changes produced by the ultrasonic waves, and all the remaining symbols have their usual meaning. The impedance (Z_s^o) depends on the acoustical displacement amplitude λ_o as well as the specific conductance (K) of the solution.

Thus
$$(Z_s^o) \cong A (P_o / \omega K) \quad (7)$$

where A is a proportionality constant and P_o is the pressure amplitude. In terms of these equations, the relative response should be linearly

dependent on the polarizing current and the pressure amplitude and inversely dependent on the frequency and the specific conductance. These relationships have been verified approximately in the experimental work.

The a. c. hydrogen electrode effect can be used for laboratory measurements of acoustical amplitude at frequencies above 100 kc./sec. where probe dimensions must be small to minimize diffraction effects. This effect may also find use in the study of the kinetics of bubble formation associated with gas electrodes.

APPENDIX

INSTRUMENTATION FOR THE DETERMINATION OF THE FREQUENCY
DEPENDENCE OF THE ACOUSTO-ELECTROCHEMICAL EFFECTS

Since one of the primary objectives of this investigation has been the determination of the frequency dependence of the various acousto-electrochemical effects, the apparatus has been designed with this objective in mind.

The apparatus involved in this investigation may be classified into three categories: (1) the variable-frequency ultrasonic generator, (2) the acousto-electrochemical cell, (3) the detection apparatus. The ultrasonic generator consists of a pulse-modulated, variable-frequency, r.-f. generator and a barium titanate transducer which serves as the source of the ultrasonic waves. The acoustical cell contains the solution under investigation in which the various a.c. effects are produced. This cell must have provisions for the transmission of the ultrasonic waves while isolating the solution within from the aqueous delay medium. The detection apparatus include the various probes and electrodes on which the alternating potentials are developed as well as the electronic apparatus necessary for the amplification and measurement of the various effects. The acoustical probes and additional equipment required for the detection of each specific effect have been presented in the previous sections on experimental data. In Figure 19 is shown a block diagram of the apparatus and associated switching network.

Pulse-Modulated, Variable Frequency Ultrasonic Generator.

The requirements for this unit are: (1) the generator must supply well-

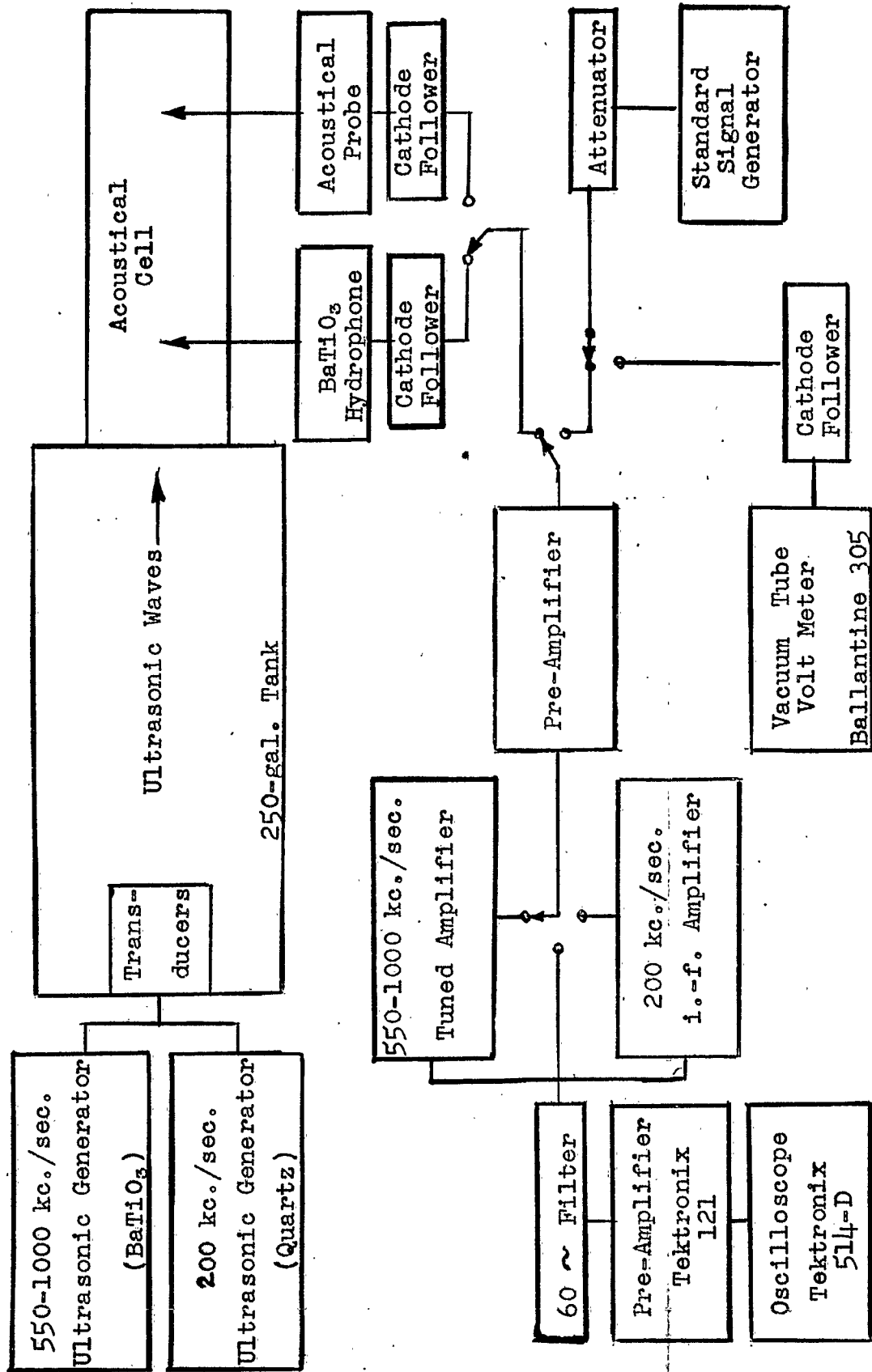


Figure 19: Apparatus for Investigation of Acousto-Electrochemical Effects: Block Diagram.

defined rectangular pulses of ultrasonic waves, (2) the pulse repetition rate and pulse duration for the modulation should be variable, (3) the acoustical output of the ultrasonic generator should be stable with respect to frequency and power, (4) the generator should be capable of producing ultrasonic waves over a frequency range of 200 kc./sec. to 1000 kc./sec., (5) the ultrasonic generator should supply instantaneous acoustical intensities of 1 watt/cm.² or more.

In Figure 20 is a block diagram of the variable frequency, pulse-modulated ultrasonic generator which has been constructed to conform to the above requirements as close as possible. Although the frequency range desired has been between 200kc./sec. and 1000 kc./sec., this unit operates most efficiently between 550 kc./sec. and 1000 kc./sec. A 200 kc./sec. ultrasonic generator¹⁰ has been available and fulfills the requirements listed above and serves to meet the lower frequency desired.

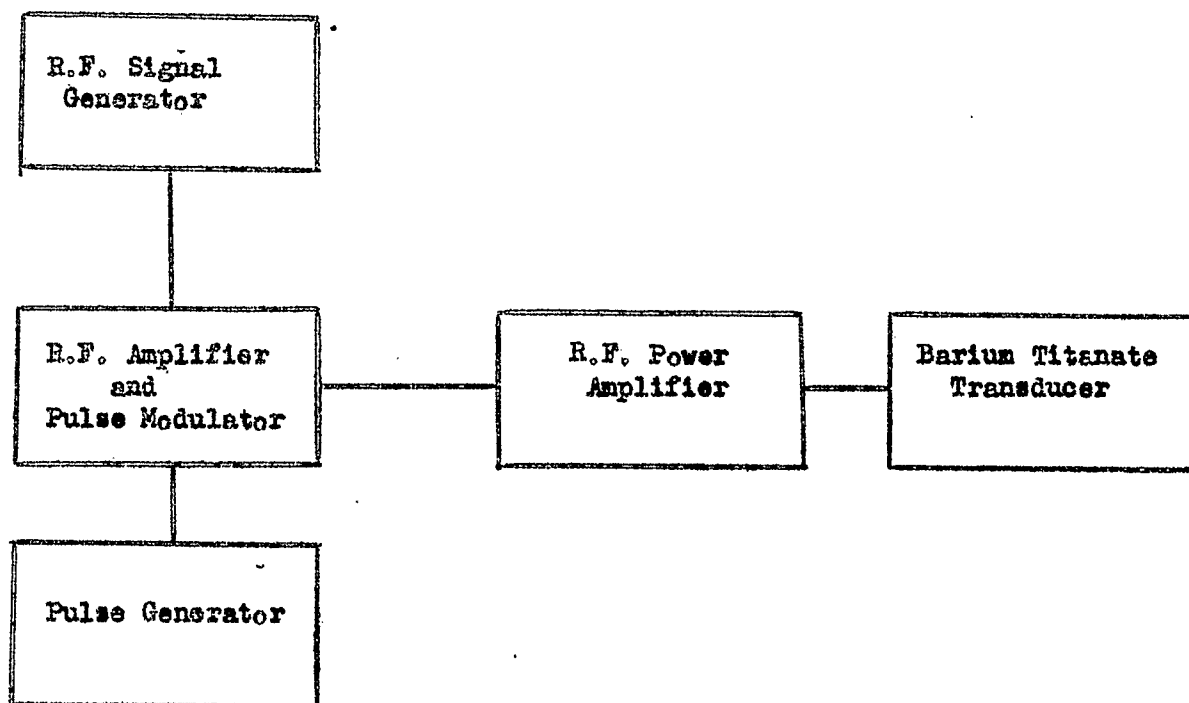


Figure 20: Variable Frequency, Pulse-Modulated Ultrasonic Generator: Block Diagram

In Figures 21-24 are shown the various circuits employed in the radio-frequency generator used to drive the barium titanate transducer. The generator consists of (1) a commercial signal generator (Precision Apparatus Co., Model E-200), modified by incorporating a cathode-follower output to ensure frequency stability with external loading, (2) a d.c. pulse generator (Figure 21) and power supply (Figure 22), (3) a pulse modulator and amplifier (Figure 23), (4) a tuned radio-frequency power amplifier (Figure 24), and (5) a barium titanate transducer and mounting (Figure 25). The frequency of the signal generator has been calibrated with a frequency meter.

The d.c. pulse generator (Figure 21) contains a multi-vibrator of variable repetition frequency, the output of which is differentiated. The resulting positive pulses are deleted by means of a diode while the remaining negative pulses are amplified and trigger a univibrator which produces rectangular pulses of controllable duration. The pulses are

introduced into the modulator circuit to pulse-modulate the radio-frequency signal. The repetition frequency is varied by a coarse (S_1) and a fine (R_5) control from 10 through 10,000 sec.⁻¹ or one-half the repetition period (whichever is shorter).

The pulse-modulator stage (Figure 23) is preceded by a radio-frequency amplifier (V_1) to increase the amplitude of the signal. Two pentagrid tubes (V_2 and V_3) serve as the pulse-modulator tubes. The radio-frequency signal is placed on the remote cut-off grid of V_2 , while the positive pulses from the pulse generator are placed on the sharp cut-off grid. This grid is normally biased to beyond cut-off. The tube V_3 in parallel with V_2 has a negative pulse placed on its sharp cut-off grid while the remote cut-off grid has no signal. The purpose of this

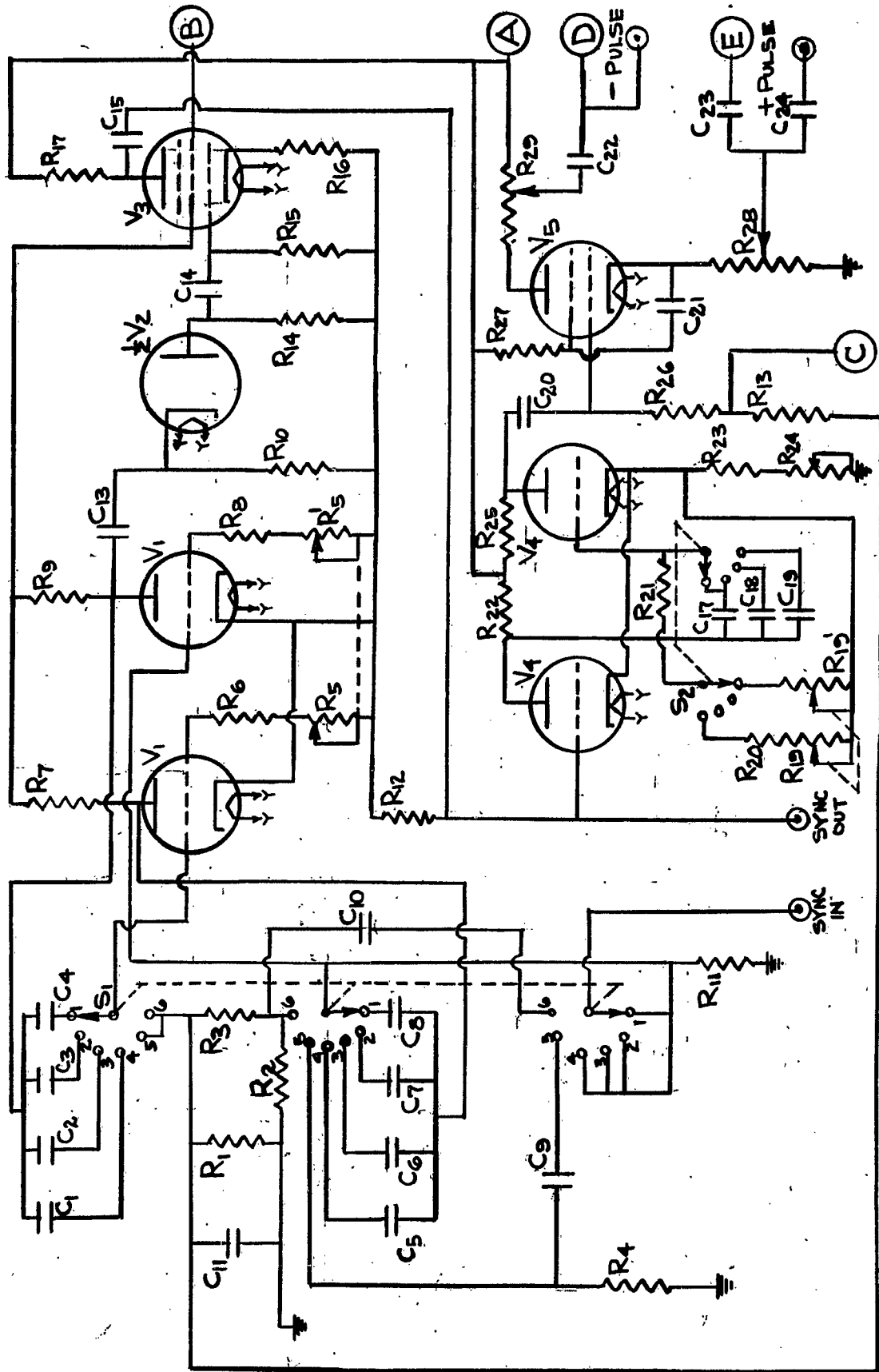


Figure 21: Pulse Generator

COMPONENT PARTS FOR PULSE GENERATOR

(Figure 21)

<u>Part No.</u>	<u>Value</u>
C1, C5	25-125 mmf.
C13	50 mmf.
C15, C16	240 mmf.
C2, C6, C17001 mf.
C3, C7, C1801 mf.
C4, C8, C11, C19, C22, C23, C241 mf.
C9, C100001 mf.
C12, C140002 mf.
C20005 mf.
C21	1 & 10 mf. (Parallel)
R1, R3, R12	51,000 ohm
R2, R13	100,000 ohm
R4	50,000 ohm
R5, R5	500,000 ohm
R6, R8, R25	15,000 ohm
R7, R11	20,000 ohm
R9	12,000 ohm
R10, R16	510 ohm
R14, R27	10,000 ohm
R15	220,000 ohm
R17	47,000 ohm
R19, R19	50,000/500,000 ohm (dual pot.)
R20	25,000 ohm
R21	250 ohm
R22	30,000 ohm
R23	1,000 ohm
R24, R28, R29	1,000 ohm
R26	500,000 ohm
V1, V4	6J6
V2	6AL5
V3	6AQ5
V5	6AQ5

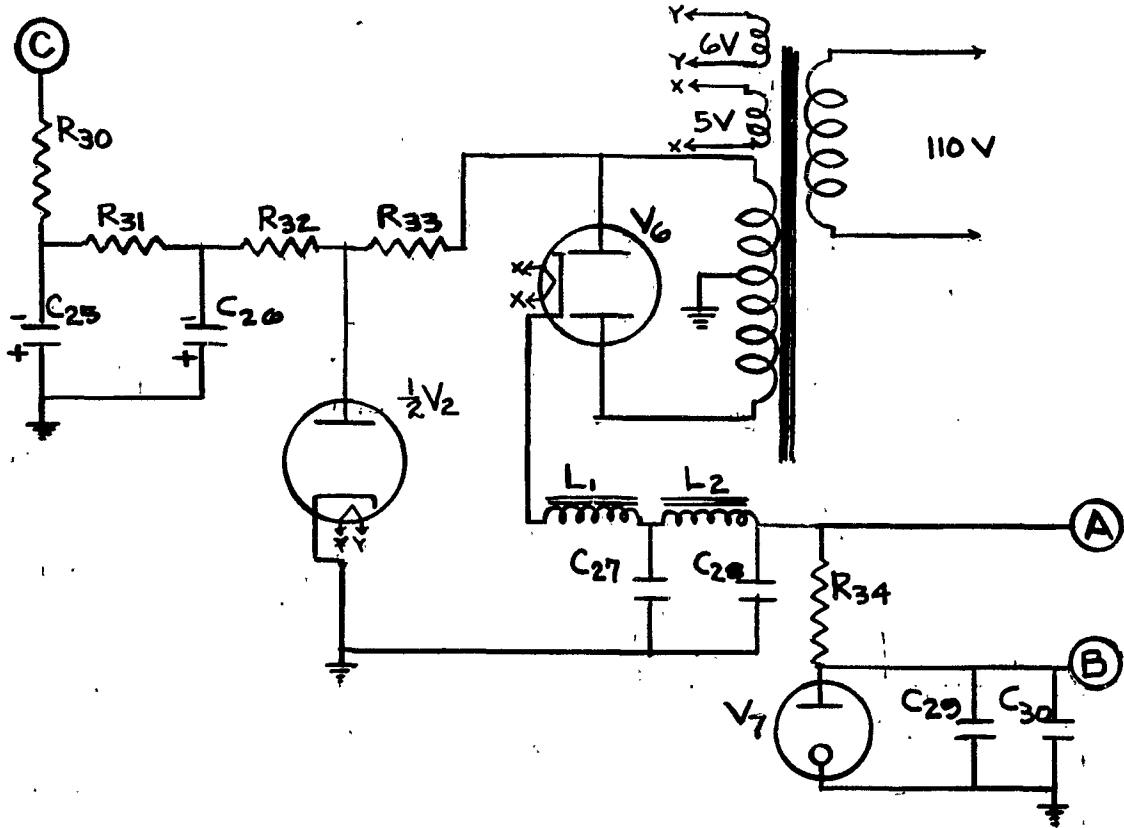


Figure 22: Power Supply for Pulse Generator

COMPONENT PARTS FOR POWER SUPPLY FOR PULSE GENERATOR

<u>Part No.</u>	<u>Value</u>
C ₂₅ , C ₂₆ , C ₂₇ , C ₂₈	20 mf. 450V.
C ₂₉	10 mf. 200V.
C ₃₀	0.1 mf.
R ₃₀	500,000 ohm
R ₃₁	50,000 ohm
R ₃₂	60,000 ohm
R ₃₃	180,000 ohm
R ₃₄	5,000 ohm
V ₆	5Y3
V ₇	0A2
L ₁ , L ₂	15 h. 100 ma.

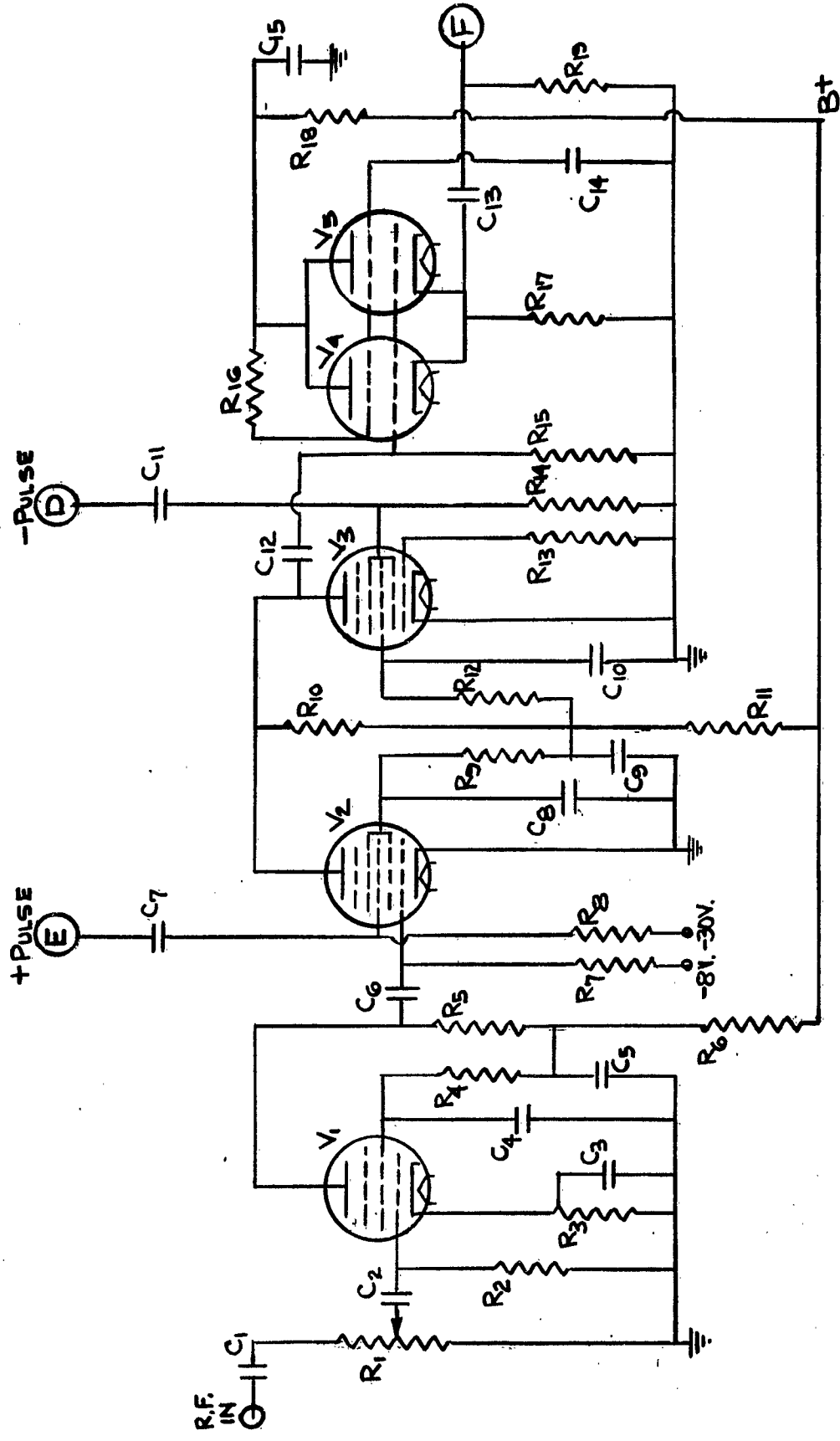


Figure 23: R.-F. Amplifier and Pulse Modulator

COMPONENT PARTS FOR PULSE MODULATOR AND AMPLIFIER*

(Figure 23)

<u>Part No.</u>	<u>Value</u>
C ₁ , C ₂ , C ₆ , C ₈ , C ₁₂01 mf.
C ₃ , C ₁₄2 mf.
C ₄ , C ₅ , C ₉ , C ₁₀ , C ₁₃1 mf.
C ₇ , C ₁₁	1 mf.
C ₁₅5 mf.
R ₁	50,000 ohm (pot.)
R ₂	500,000 ohm
R ₃ , R ₁₉	200 ohm
R ₄	4,000 ohm
R ₅ , R ₁₀	5,000 ohm
R ₆	12,000 ohm
R ₇ , R ₁₃	100,000 ohm
R ₈ , R ₁₄ , R ₁₅	50,000 ohm
R ₉ , R ₁₂	6,000 ohm
R ₁₁	10,000 ohm
R ₁₆	15,000 ohm
R ₁₇	300 ohm
R ₁₈	400 ohm
V ₁	6AK5
V ₂ , V ₃	6L7
V ₄ , V ₅	6L6

* A commercial power supply (Zenith, No. 4A86) has been used to supply plate voltage for this unit. A filament transformer has been incorporated with the power supply to provide filament voltage. The bias voltage is obtained from the pulse generator power supply.

arrangement is to eliminate the d.c. pulse by placing oppositely directed voltage pulses simultaneously on the grids of the two tubes with a common plate resistor. The radio-frequency pulses are amplified by two beam-power tubes (V_4 and V_8) in parallel with by a cathode-follower output to the power amplifier.

The power amplifier (Figure 24) is a conventional radio-frequency amplifier with two tuned stages. All components are well shielded to eliminate oscillations and feed back. Fixed bias has been used on all stages to minimize changes in grid bias with pulse length. The bias voltage may be adjusted by R_4 and R_5 . The final stage is link-coupled to the barium titanate transducer. A two position switch is employed in the output to provide adequate matching for the transducer over the frequency range used.

The transducer consists of a 2-in. diameter barium titanate ceramic disc with a resonate frequency (thickness mode) of 1 mc./sec. It has been mounted in a brass housing shown in Figure 25. The constituent parts of the housing are held together by soldered joints except for the back plate which is bolted to the housing through a rubber gasket. The barium titanate element is held in place by a shoulder in the front plate and a circular contact ring mounted in a plastic disc. The brass contact ring serves as an electrical contact between the silvered surface of the transducer and the lead-in wire. The plastic disc which holds the contact ring is held firmly in place by a tension screw which is threaded through the center of a circular brass fitting. This brass plate is screwed into the main housing and serves as a stop for the tension screw. The front surface of the transducer is coated with silver conducting paint to make contact with the brass housing which serves as the ground

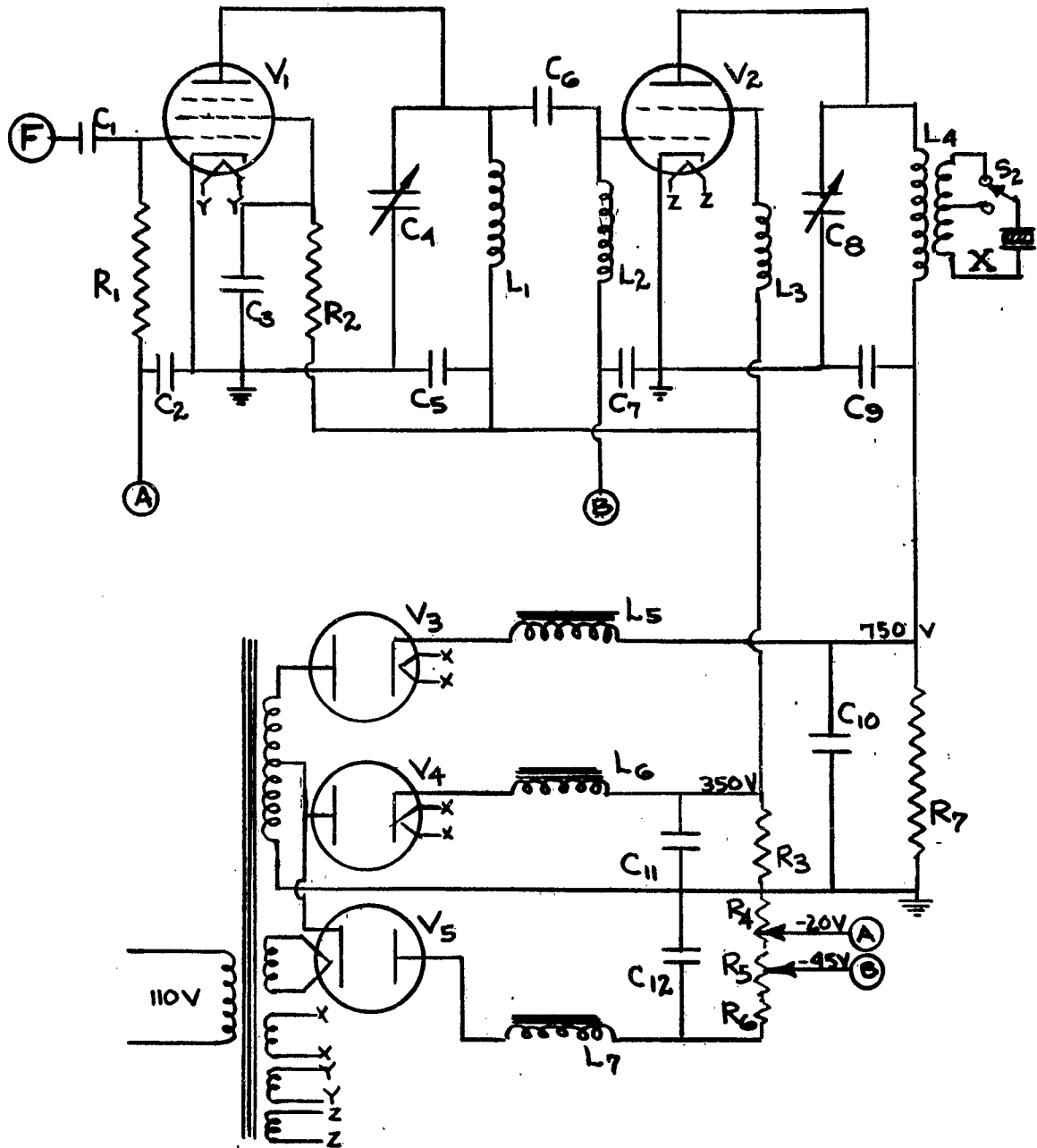


Figure 24: Power Amplifier

COMPONENT PARTS FOR POWER AMPLIFIER

(Figure 24)

<u>Part No.</u>	<u>Value</u>
C ₁ , C ₂ , C ₃ , C ₅ , C ₆ , C ₇ , C ₉01 mf.
C ₁₀ 1	10 mf. (1000V)
C ₁₁ , C ₁₂	8 mf. (500V)
C ₄ , C ₈	200 mmf. (Variable)
R ₁	50,000 ohm
R ₂	5,000 ohm
R ₃	30,000 ohm
R ₄	10,000 ohm (Pot.)
R ₅	50,000 ohm (Pot.)
R ₆	20,000 ohm
R ₇	80,000 ohm
L ₁ , L ₄	1,000 mh.
L ₂ , L ₃	20 mh.
L ₅ , L ₆ , L ₇	10 h.
X	Barium Titanate Transducer (1 mc. resonant freq.)
V ₁	6L6
V ₂ 1	807
V ₃	6W4
V ₄ , V ₅	6X4

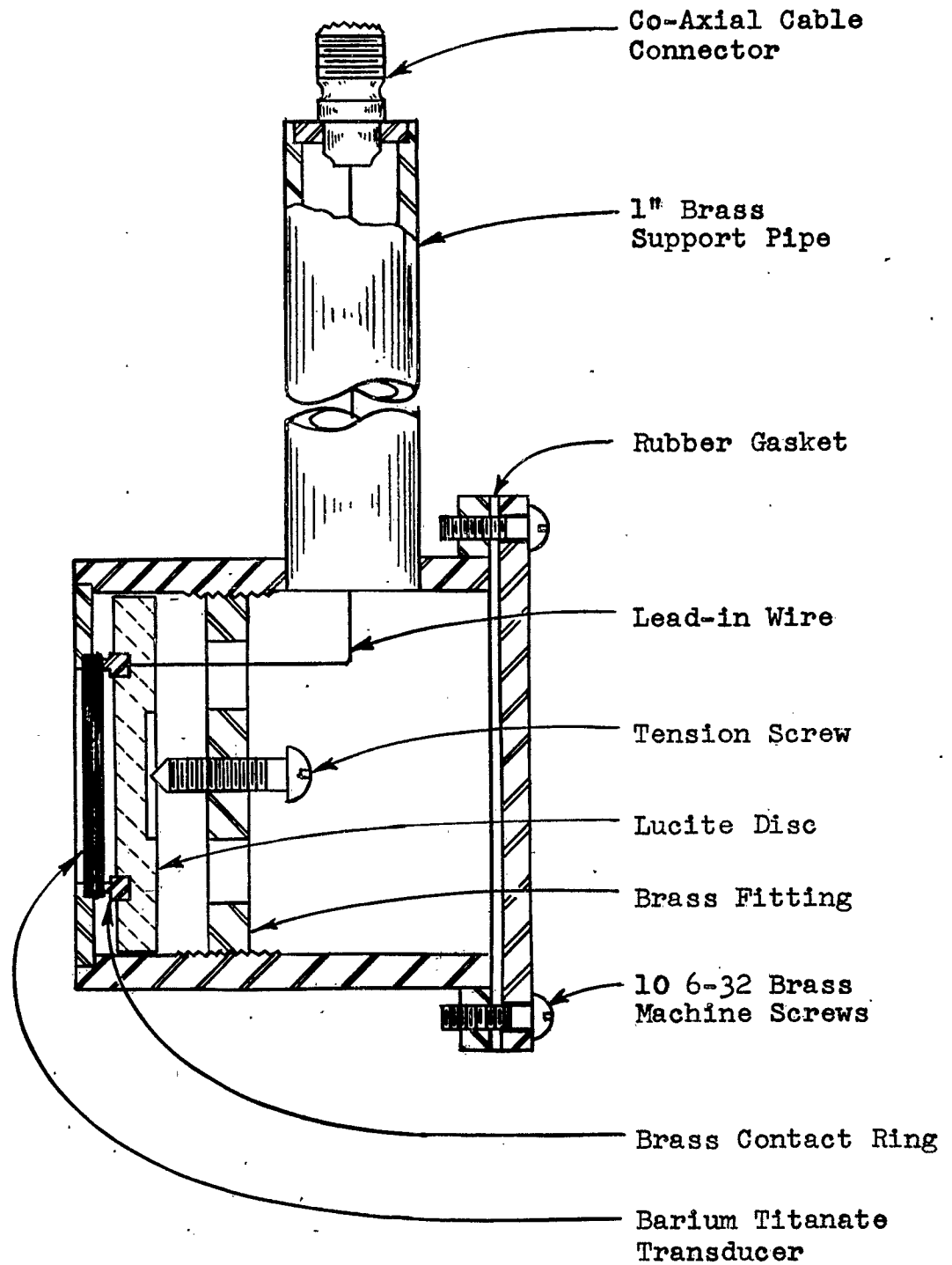


Figure 25: Transducer Mounting

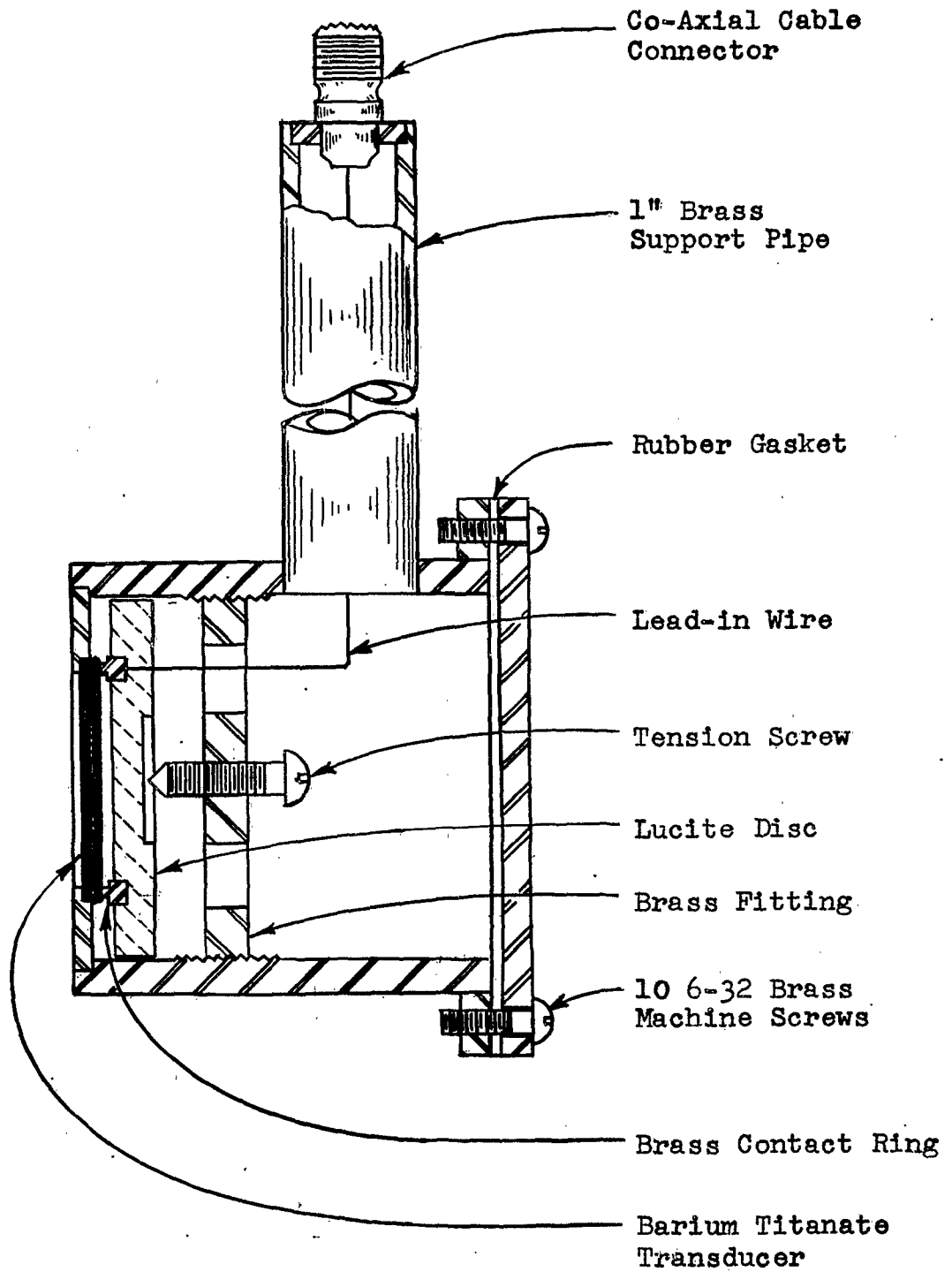


Figure 25: Transducer Mounting

connection. The entire housing is coated with Tygon paint and the support pipe is nickel plated.

The transducer mounting has been suspended in a 250-gallon thermostated tank¹⁰ by means of a specially constructed aluminum alloy support. The transducer may be positioned vertically and horizontally in the direction of propagation. The desired positions are maintained by suitable positioning locking screws. Figure 26 is a drawing of the ultrasonic propagation system. The barium titanate transducer can be seen suspended in the 250-gallon tank. Immediately behind the barium titanate transducer is the 200 kc./sec. quartz transducer used in conjunction with the 200-kc./sec. ultrasonic generator.

Acousto-Electrochemical Cell. -- The main criteria in the design of the acousto-electrochemical cell has been to have minimum attenuation and scattering of the ultrasonic waves propagated into the cell. In the previous work at 200 kc./sec., the acoustical cell consisted of a thin glass vessel in the shape of a bulb. This type of cell is unsatisfactory for work at higher frequencies due to the excitation of various radial modes of the spherical vessel and interfering reflections from the back surface. At frequencies of 1 mc./sec., the interference and scattering of the ultrasonic waves as observed with a barium titanate hydrophone placed in a cell showed that quantitative measurements would be difficult.

The acoustical cell that has been used in this investigation consisted of an 8-in. diameter plastic tube, 33 in. long with 3/8-in. walls. This tube has been mounted on one end of the 250-gallon tank as shown in Figure 26. The end of the cell which is fastened to the tank

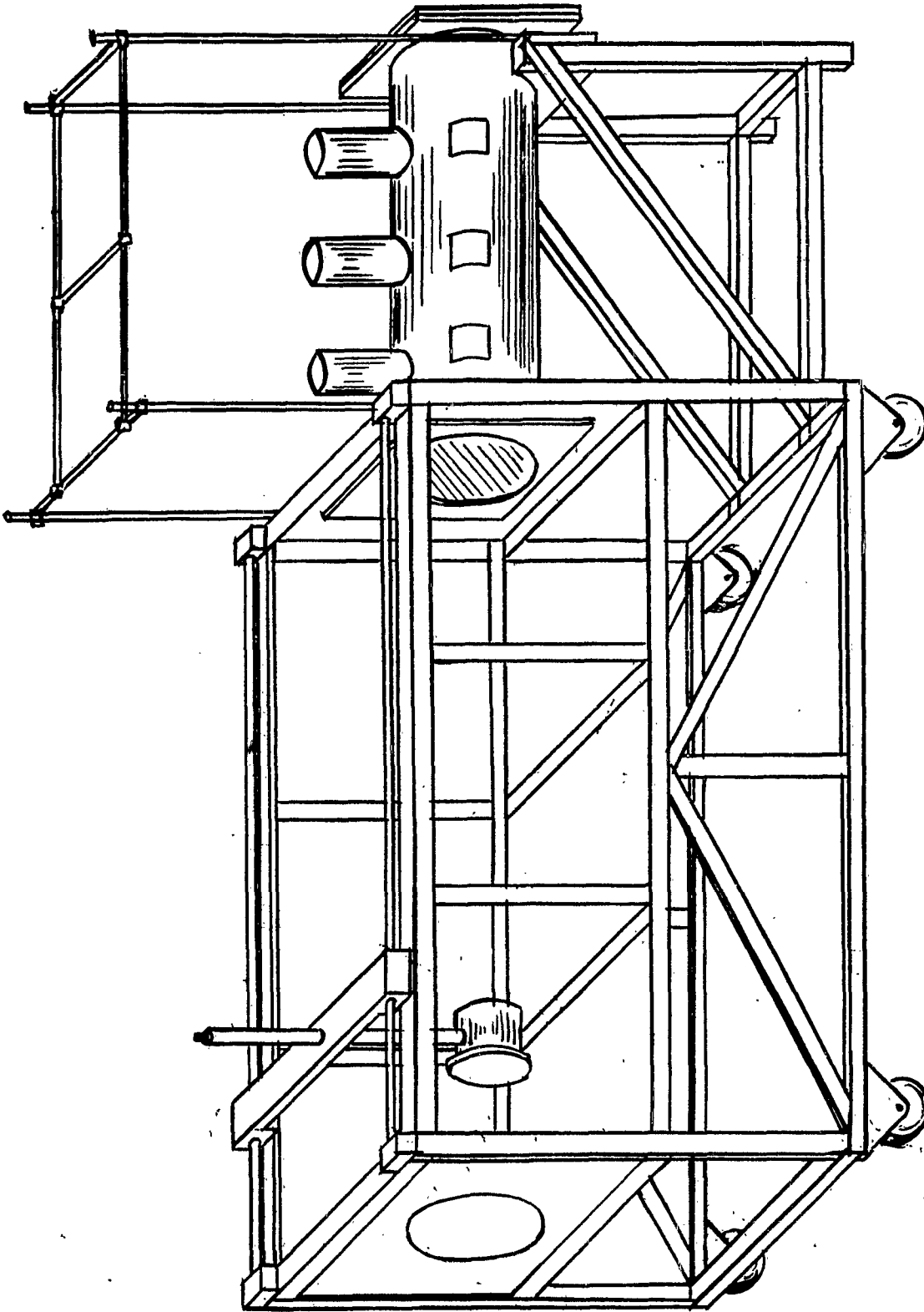


Figure 26: Propagation System for the Study of Acousto-Electrochemical Effects

protrudes into it one inch and a 1/4-in. thick rho-c rubber diaphragm has been fastened over the open end to isolate the water in the tank from the contents of the cell. A 1/16-in. plastic plate has also been used as an acoustical window with very little attenuation of the ultrasonic waves. The other end of the cell has been sealed with a plastic flange plate cemented to the cell. On the top of the cell three plastic tubes, 8 in. in length and 2 in. in diameter with 1/4-in. walls, have been placed. These tubes serve as entrance ports to the solution contained in the cell. The entire cell has been covered with a copper foil to provide shielding from stray radiations and electromagnetic pick-up from the ultrasonic generator. The capacity of the cell is approximately 30 liters.

The various detection probes were held by a support rack constructed over the cell mounting. The cell was mounted in a cradle support and rigidly secured to the framework of the tank.

A variable speed stirrer has been placed in one of the ports to provide adequate stirring of the solution. The temperature was controlled by an immersion heater enclosed in a glass tube containing transformer oil as a heat transfer medium. A plastic reflector, at an oblique angle, has been placed in the last port behind the acoustically sensitive probe. This permitted the pulses to be scattered after producing the desired effect and thus eliminated possible interference by reflected pulses from the end of the cell.

The advantages of this construction for the acoustical cell are the relatively uniform sound field over the frequency range considered, and the additional delay time offered by the increase in the acoustical path length. This latter advantage permitted the use of longer pulse widths

which improved the performance of the tuned stages used in the detection apparatus.

Detection Apparatus. -- The detection of the various a.c. acousto-electrochemical effects depends upon the amplification of the acoustically produced effect and determination of the magnitude of effect in terms of the intensity of the ultrasonic waves.

A barium titanate hydrophone¹⁰ has been used to measure acoustical pressure amplitudes of the ultrasonic waves propagated through the acoustical cell. The construction of the hydrophone is shown in Figure 27. The sound sensitive element is a 1/8-in. diameter radially-polarised barium titanate ceramic cylinder, 1/8-in. long. The element is held in a plastic mount at the end of a tubular probe housing as shown in Figure 27. The response of the hydrophone that has been used in this investigation has been compared with a hydrophone of similar construction that has been calibrated by the U. S. Navy Underwater Sound Reference Laboratory at Orlando, Florida. The response is not linear with frequency due to the excitation of the various vibrational modes of the ceramic element. The frequency points that have been used for the frequency dependency data are situated at points in the hydrophone calibration curve where there is no abrupt change in the response. The frequency calibration of the monitoring hydrophone has been done with the variable-frequency ultrasonic generator previously described. The two hydrophones have been positioned in the sound field by means of a positioning mechanism constructed over the 250-gallon tank. The response of the monitoring hydrophone has been calculated in terms of the calibrated hydrophone in db. relative to one volt per dyne/cm.²

The detection system for the acousto-electrochemical effects includes the probe on which the a.c. components are developed, a pre-amplifier,

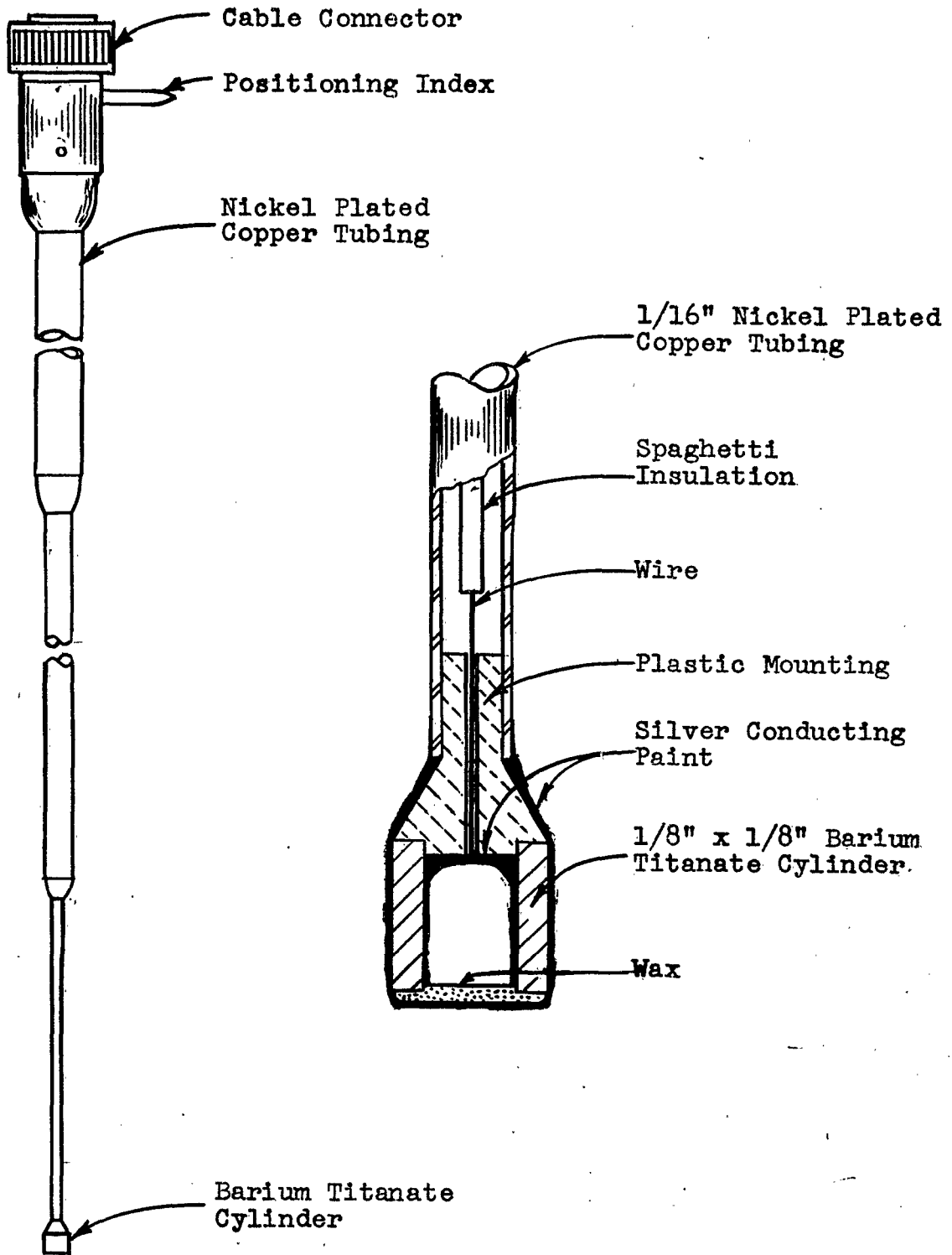


Figure 27: Barium Titanate Hydrophone

an intermediate-frequency amplifier, an oscilloscope, and a standard signal generator. The a.c. components are first introduced into a cathode follower, followed by a pre-amplifier similar in design to that of a Ballantine vacuum tube voltmeter, Model 305. The amplified signal is then fed to a modified Hallicrafter commercial receiver, Model SX 200, to amplify further the signal in the frequency range of 550 kc./sec. to 1000 kc./sec. The 200 kc./sec. signal is passed through a multi-stage intermediate-frequency amplifier consisting of one stage at 200 kc./sec. and two stages at 456 kc./sec. The output from the i.-f. amplifier is examined with a Tektronix oscilloscope, Model 514 D, in conjunction with a Tektronic pre-amplifier, Model 120.

The response from the barium titanate hydrophone is also sent through a cathode follower stage and then by means of a junction switching box through the same amplification circuits as the detected a.c. effect. A selector switch in the junction box permits the signal to by-pass the tuned i.-f. circuits. This permits the investigation of the structure of the pulses exclusive of any tuned stages when the signal is of sufficient amplitude.

The magnitude of the pulse-modulated signals from the probe as well as the response from the barium titanate hydrophone have been measured by the substitution method with a General Radio standard signal generator, Model 805-C, as the source of known r.-f. voltage. This calibrating voltage is introduced into the junction switching box where it is sent through the same amplification stages as the observed signal. The frequency of the voltage standard is carefully adjusted to zero beat with the carrier of the pulse-modulated ultrasonic waves.

By comparing the voltages of the a.c. effect and that of the barium titanate hydrophone placed in the cell, the magnitude of the effect can be calculated in terms of the intensity of the ultrasonic waves and converted to a convenient reference standard.